The Company of
Biologists

RESEARCH ARTICLE

Functional morphology of tarsal adhesive pads and attachment ability in ticks *Ixodes ricinus* (Arachnida, Acari, Ixodidae)

Dagmar Voigt*,‡ and Stanislav Gorb

ABSTRACT

The presence of well-developed, elastic claws on ticks and widely pilose hosts led us to hypothesise that ticks are mostly adapted to attachment and locomotion on rough, strongly corrugated and hairy, felt-like substrates. However, by using a combination of morphological and experimental approaches, we visualised the ultrastructure of attachment devices of *Ixodes ricinus* and showed that this species adheres more strongly to smooth surfaces than to rough ones. Between paired, elongated, curved, elastic claws, *I. ricinus* bears a large, flexible, foldable adhesive pad, which represents an adaptation to adhesion on smooth surfaces. Accordingly, ticks attached strongest to glass and to surface profiles similar to those of the human skin, generating safety factors (attachment force relative to body weight) up to 534 (females). Considerably lower attachment force was found on silicone substrates and as a result of thanatosis after jolting.

KEY WORDS: Adhesion, Human skin, Resilin, Roughness, Safety factor, Traction force

INTRODUCTION

Attachment of ticks has been frequently related to the fixation of their mouthparts to the host skin (Lees, 1948; Wallade and Rice, 1982; Sauer et al., 1995; Voltzit, 1996; Grenacher et al., 2001; Buczek and Bartosik, 2006; Allan, 2010; Francischetti et al., 2010; Heinze et al., 2012; Wilhelmsson et al., 2013; Sonenshine and Roe, 2014a). But before a blood meal, they have to seek hosts and find suitable sites on the host to penetrate (Schmalfuss, 1994). Besides residing on a wide range of vertebrate hosts, *Ixodes ricinus* L. (Arachnida, Acari, Ixodida, Ixodidae) spends more than 90% of its 0.5–3 year lifetime off hosts in the litter and on diverse plants including grass, herbs and ferns (Enigk, 1953; Babos, 1964; Cheng, 1973; Crooks and Randolph, 2006; Healy and Bourke, 2008). In order to ambush hosts, ticks periodically move up and down plants, covering distances of up to 9 m at a speed of up to 5.5 cm min^{-1}, searching for suitable questing sites (Lees, 1969; Hackman and Filshie, 1982; Alekseev et al., 2000; Perret et al., 2003; Crooks and Randolph, 2006; Sonenshine and Roe, 2014b). The question arises: how do ticks attach their feet and walk?

The transition of ticks from plants to hosts has been described as: (1) slough off/fall off, (2) catches hold, (3) climbs on and

Department of Functional Morphology and Biomechanics, Zoological Institute, Christian-Albrechts-Universität zu Kiel, Am Botanischen Garten 1–9, Kiel D-24098, Germany.
*Present address: Institute for Botany, Technische Universität Dresden, Dresden D-01062, Germany.

‡Author for correspondence (dagmar.voigt@tu-dresden.de)

D.V., 0000-0003-2772-8504

(4) clamping behaviour (Lees, 1948; Schmalfuss, 1994; Liebisch and Liebisch, 2003). Upon arrival on the host, they hold and cling on tenaciously, and migrate over the body by active walking with a speed of up to 4.5 mm s^{-1} on pilose mice and 2 mm s^{-1} on the human body (MacLeod, 1932; Lees, 1948; Nilsson and Lundqvist, 1978; Schmalfuss, 1994; Alekseev and Dubinina, 2006; Allan, 2010). Locomotion is realised by four pairs of walking legs, which look similar in all four life stages of the hemimetabolous ticks, whereas larval stages bear only three pairs of legs (Sonenshine and Roe, 2014a). Each leg consists of six podomeres connected by a soft articulation membrane: coxa, trochanter, femur, patella, tibia, tarsus (Coons and Alberti, 1999; Sonenshine and Roe, 2014a). Terminally, a large, globular, foldable structure, previously named pulvillus, arises adjacent to the paired, tapered claws, and facilitates walking and climbing on various surfaces, particularly on smooth ones (Pagenstecher, 1861; Falke, 1931; Babos, 1964; Baker, 1997; Sonenshine and Roe, 2014a). This pad consists of three lobes held together by a thin membrane and is well developed in both sexes of *I. ricinus*, being distinctly largest on first tarsi (Ruser, 1933; Babos, 1964; Buczek et al., 2004).

If the pretarsus lifts from the ground, ventrally curved claws turn to the side-by-side configuration, folds of pulvillus become deeper, and the pulvillus collapses. During contact formation with the ground, the claws spread apart, and the pad becomes wider as a result of unfolding and smoothening presumably caused by haemolymph pressure (Babos, 1964).

Gripping the host with their legs, ticks lift their body at an angle to the surface, forcing the capitulum against the surface of the host's integument, inserting the hypostome (Kemp et al., 1982; Wallade and Rice, 1982; Voltzit, 1996; Liebisch and Liebisch, 2003; Sonenshine and Roe, 2014a). A reliable foothold is required in at least five life situations of *I. ricinus*: (1) while walking and questing on banker plants, (2) when transferring from plants to vertebrate hosts, (3) while walking on hosts seeking feeding sites, (4) while supporting the hypostome anchor into the skin, and (5) during mating.

Taking into account the off- and on-host life strategy of *I. ricinus*, accessing a broad range of banker plants and vertebrate hosts, ticks should be able to attach their feet to a tremendous variety of surfaces (Fig. 1), spanning smooth and rough, irregular and regular, non-wavy and wavy, non-structured and structured, wettable and non-wettable, and even the water–oil emulsion (antibiotic, acidic hydrolipid film composed of sweat and sebum) covering the polymorphic human skin (Igarashi et al., 2005; Derler and Gerhardt, 2012). In addition, ticks must overcome such challenges as the transition from plants to motile hosts, withstanding host movements and grooming, and the 135-fold multiplication of body weight from the unfed to the fully fed female (Arthur, 1945; Oliver, 1989; Uspensky et al., 1999; Liebisch and Liebisch, 2003). How do ticks cope with these requirements and a heterogeneous environment? Do they rely on specific tarsal attachment strategies?
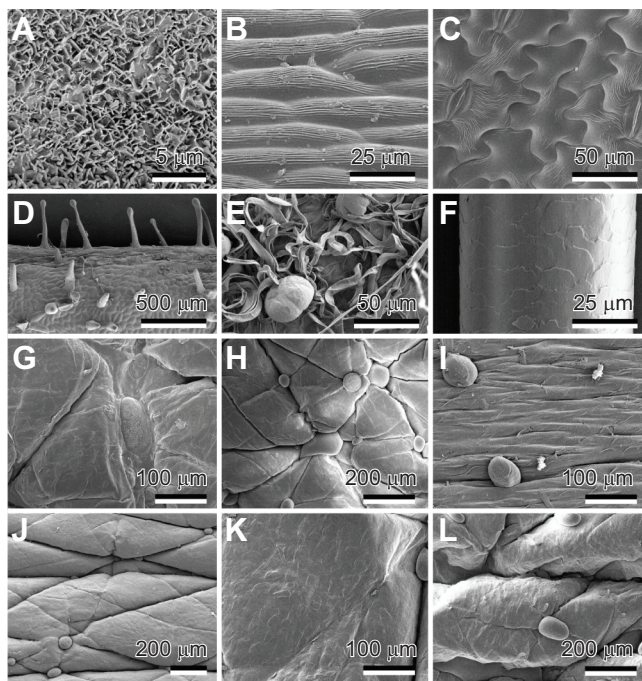
Fig. 1. Examples of plant and human substrates accessed by *Ixodes ricinus* (SEM and cryo-SEM images). (A) Leaf lamina of *Deschampsia flexuosa* (Poaceae) covered with crystalline wax plates. (B) Adaxial flower surface of *Trifolium pratense* (Fabaceae) showing parallel cuticular folds on convex epidermal cells. (C–E) Abaxial leaf surfaces of *Vicia faba* (Fabaceae) characterised by undulate, convex epidermal cells (C), *Rumex obtusifolius* (Polygonaceae) main vein covered with glandular and non-glandular trichomes (D), and *Arctium tomentosum* (Asteraceae) with a felt-like pubescence and several peltate trichomes (E). (F) Hair from a female human head (*Homo sapiens*, Primates, Hominidae). (G–L) Resin replicas of 30 year old female human skin, demonstrating varying surface texture within one host individual: the elbow pit/cubital fossa (G); the armpit/ventral axilla (H); the back of the head behind the ear (I); the lateral hip (J); the hollow of the kull/politeal fossa (K); and the ventral ankle (L). Note the shape of the skin microfolds, pores and sweat drops.

To study the functional morphology of the tick attachment system in detail, we combined microscopic analyses and force measurements. The following experiments were carried out, analysing attachment ability under three different conditions and postures on various substrates. (1) Inversion tests allowed the screening of attachment on 14 surfaces varying in their roughness and wettability. Immobile, non-feeding, attached ticks were suddenly rotated from the horizontal upright to the horizontal ceiling position. Such an event may happen in the field, e.g. when leaves with attached ticks are bent by the action of the wind. Then, animals rely on adhesion and/or grasping rather than shearing and friction by the feet. (2) Centrifugal force tests were applied to measure maximum friction forces of ticks as they slip along the surface while rotating. The horizontal situation of test individuals on the centrifuge drum is partially comparable to the situation when the animal attaches to vertical substrates in the field. By using this technique, we compared the attachment of males and females on differently wettable surfaces: hydrophilic (normal) and hydrophobic (silanised) glass. (3) Traction force measurements were used to provide force data, obtained from actively horizontally walking and tracking females. This situation best resembles the attachment to a host; however, the experimental substrate was fixed during the experiment, which is of course different from the real situation, when the host body is in motion. As males are less important ectoparasites

and difficult to handle because of their small body size, they were not considered in inversion and traction tests. Pilose substrates were neglected in experiments because ticks have previously been observed on large vertebrates mostly walking in between hairs and touching only the hair-free spaces with their legs (D.V., personal observation). We assumed roughness and wettability to be the main surface features influencing tick attachment. Hence, we mainly focused on these aspects in the present study.

MATERIALS AND METHODS
Ticks
Not engorged, questing adult *I. ricinus* were collected from various herbaceous plants at a roadside, grassed area in Stuttgart-Büsnau, Germany (48°44′5″N, 9°4′54″E), and kept in ventilated plastic boxes on moist filter paper at 23±2°C, 75±5% relative humidity and a light photoperiod of 16 h day^{-1}, for not longer than 3 days.

Microscopy
Detailed information about the attachment system was obtained from light microscopy, fluorescence microscopy, transmission electron microscopy (TEM) and cryo-scanning electron microscopy (cryo-SEM).

Light microscopy
An Olympus SZX16 stereomicroscope combined with Olympus SDF Plapo 1.6xPF and 0.5xPF objective lenses, an Olympus DP26 camera and CellSens Standard software (Olympus Corp., Tokyo, Japan) were used to observe male and female *I. ricinus* in motion, and obtain images and video sequences.

Additionally, tarsi of anaesthetised adult ticks were cut off with a razor blade, mounted on glass slides in polyvinylalcohol Mowiol® 4-88 (Sigma-Aldrich Co. LLC), covered with glass coverslips and observed in a Zeiss Axioplan fluorescence microscope, equipped with an HBO 103 mercury vapour lamp and XBO 75 xenon shortarc lamp (Carl Zeiss MicroImaging GmbH, Jena, Germany) as well as an integrated digital video-camera (AxioCam MRc, AxioVision GmbH, München-Hallbergmoos, Germany). Fluorescence microscopy was used to localise the auto-fluorescent elastic protein resilin in the pretarsus (Andersen and Weis-Fogh, 1964; Gorb, 1999).

Cryo-SEM
A cryo-SEM Hitachi S-4800 (Hitachi High-Technologies Corp., Tokyo, Japan) equipped with a Gatan ALTO 2500 cryo-preparation system (Gatan Inc., Abingdon, UK) was used. Fresh samples of tick legs were cut using a razor blade, mounted on metal holders with adhesive fluid (Tissue-Tek® O.C.T.™ Compound, Sakura Finetek Europe B. V., Zoeterwoude, The Netherlands), frozen in the preparation chamber at −140°C, sublimated for 3 min at −90°C to remove contamination in the form of condensed ice crystals, sputter-coated with gold–palladium (6 nm thickness) and examined in a frozen state in the cryo-SEM at 3 kV and −120°C. To visualise pretarsi attached to substrates and footprints after detachment, feet were carefully brought in contact with gold–palladium-coated resin replicas of either glass or skin of female human lower forearm and examined as described above (for detailed description, see Gorb, 2006; Gorb et al., 2012).

TEM
Tarsi were fixed for 12 h at 4°C in 2.5% glutaraldehyde (in 0.01 mol l^{-1} phosphate buffer at pH 7.3), and post-fixed for 1 h in 1% osmium tetroxide in phosphate buffer at 2°C. After washing, preparations were stained for 1 h at 4°C in 0.1% aqueous uranyl

acetate solution, washed, dehydrated and embedded in a low-viscosity resin (Spurr, 1969). Ultrathin sections were picked up on copper grids coated with formvar film. Sections were stained with uranyl acetate and lead citrate, and observed with a Philips CM10 transmission electron microscope (Philips Electron Optics, Eindhoven, The Netherlands) at various voltages and magnifications.

Morphometrical evaluation

Measurements of pretarsal components were carried out using microscopic images and micrographs of 5–10 randomly selected pretarsi of adult specimens and Sigma Scan Pro 5 software (SPSS, Inc., Chicago, IL, USA).

Attachment experiments

Inversion test

Tick attachment was tested on glass, silicone and Spurr resin replicas of the skin of a 30 year old human female ventral forearm as well as on Spurr resin surfaces of defined roughness, obtained from mouldings of polishing paper (see Gorb, 2007b, for the moulding technique). Skin replicas were obtained from native skin of D.V., who was fully informed and voluntary. The roughness average (R_a) of surface asperities was measured using the profilometer Veeco Dektak® 8 (Veeco Instruments, Inc., Tucson, AZ, USA). For contact angle measurements and estimation of the free surface energy (FSE) of test substrates, see Table S1.

A tick specimen was placed on the test surface, and the surface then inverted 180 deg within 1 s. This procedure was done manually and smoothly at the same speed in all tests, avoiding variations that affected the results.

The attachment ability was categorised as fall off (no attachment) and attachment. For each surface, 10 females were tested. The sequence of 14 test surfaces was varied randomly. A total of 1400 individual inversions (N=10 females, n=10 inversions per female per surface) were carried out at 23±2°C and 55±3% relative humidity. Data were analysed by contingency tables (SigmaStat 3.1.11 software, Systat Software Inc., Richmond, CA, USA).

Centrifugal force test

To assess attachment forces on normal and silanised glass discs, the computer-controlled centrifugal force tester Tetra Zentri-01-P (Tetra GmbH, Ilmenau, Germany) was applied (see Gorb et al., 2001, for the procedure). Prior to experiments, glass was cleaned, hydrophobised, and characterised according to Voigt and Gorb (2010) (Table S1).

Each tick was weighed using an analytical balance (AG 204 Delta Range, Mettler Toledo GmbH, Greifensee, Switzerland). Individual adult *I. ricinus* were placed on the horizontal surface of the centrifuge drum, which was covered with the glass substrate, and accelerated from 50 to 3000 rpm (0.14 to 540 *g*) in 20 s; 25 males and 25 females were tested once per test surface. The sequence of the different substrates was randomly changed during the experiment. In total, 100 individual tests were conducted under laboratory conditions of 23.7±1.7°C and 47.3±10.0% relative humidity. Mann–Whitney rank sum test was used to elucidate differences in the friction force and safety factor values (friction force normalised by the tick's weight) between (1) males and females and (2) normal and silanised glass (software SigmaStat 3.1.11).

Traction force test

Traction force measurements were carried out according to Gorb et al. (2004) and Voigt et al. (2007). Ticks were individually

weighed using the analytical balance (AG 204 Delta Range) and attached to a 10 cm-long human hair with a molten wax droplet on their scutum. The free end of the hair was connected to a force sensor (FORT-10, 10 g capacity, Biopac Systems Ltd, Santa Barbara, CA, USA). Test surfaces were attached to a horizontal glass plate using double-sided tape. Each tick was tested walking horizontally on normal glass, resin and silicone replicas of skin as well as on the living native skin of the ventral forearm of a 30 year old female human (for contact angle and FSE, see Table S1). The test person was D.V., who was fully informed and voluntary; she did not use any perfume, nor did she drink any tea or coffee (or take any other drugs) on the day on which experiments were carried out. The succession of different substrates (1–4) was randomly organised during the experiment. Using AcqKnowledge 3.7.0 software (Biopac Systems Ltd), force–time curves were recorded to estimate the maximal and average traction force generated by a single tick during five consecutive runs on a test substrate. On each surface, 10 females were tested individually. In total, 200 individual tests were carried out (N=4 substrates, n=10 females, 5 runs per female). Kruskal–Wallis one-way ANOVA on ranks followed by all pair-wise multiple comparison procedures (Tukey test) was applied to determine differences in force between test surfaces (SigmaStat 3.1.11 software). For laboratory conditions see 'Centrifugal force test', above.

RESULTS

Legs and posture

Legs appeared to be highly flexible because of their elastically articulated segments, all roughly similar in length and width (Fig. 2; Table S2). They were mostly held arcuately curved, and could be instantly folded tightly to the ventral body after a disturbance (thanatosis) and during quiescence. During waving and questing with the forelegs, the three remaining pairs of legs were used for locomotion and provided sufficient hold while walking horizontally, upside-down on the ceiling and vertically up and down (Fig. 2A). The forelegs were observed to contact the passing host first for transition from plants. On human skin, ticks moved without hindrance, spanning several skin microfolds with their legs (Fig. 2B,C). In the ceiling situation (upside-down position), female *I. ricinus* walked at a velocity of up to 2.3 mm s^{-1} on glass using four pairs of legs for locomotion (Movie 1). Three pairs of legs generated sufficient adhesion while resting (Fig. 2D).

On rod-shaped substrates, such as plant stems and bundles of hairs, arcuate legs entirely surrounded the substrate, supporting clinging and climbing.

Tarsal morphology

Corresponding to previous reports (Babos, 1964), each leg terminated with an ambulacrum (pretarsus), which was composed of an elongated apotele bearing long, paired, rod-shaped, curved claws (Figs 2E–G and 3A,E). They appeared lunate and transparent, having an average thickness of 15.1±1.31 μm (n=5) and a length of 135.2±17.58 μm (n=5). A thin outer cuticular layer surrounded the claw interior, which was completely filled with an amorphous material (see below). They tapered into a mean claw tip diameter of 1.2±0.36 μm (n=10). The claw base was slightly broadened, reaching about 20.1±1.62 μm in width (n=5). The mean diameter of a circle fitting the claw curvature measured 54.7±8.08 μm (n=10). Between the claws, a foldable pad arose (Figs 2E–G and 3A–D). The fluorescence microscopy images (Fig. 2F,G) revealed the presence of resilin, an elastic protein, in the materials of pads, claws and membranous areas surrounding the tarsal–pretarsal articulation.
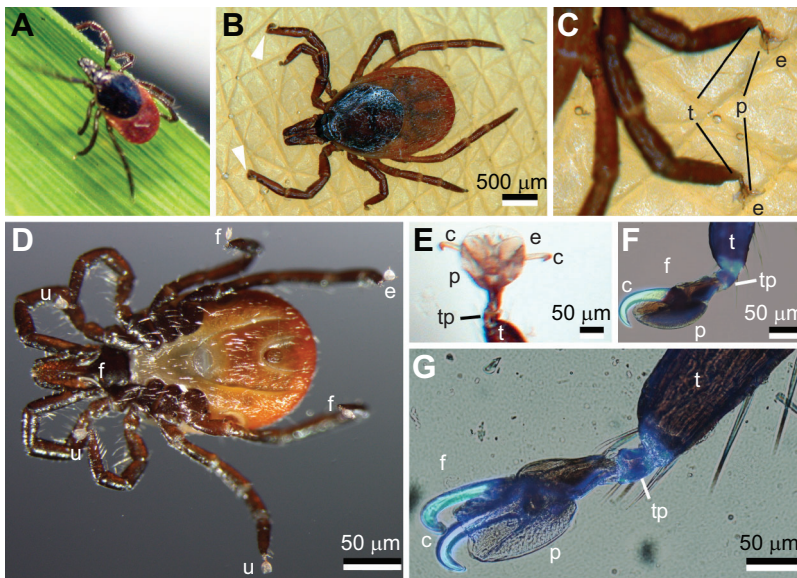
Fig. 2. Light microscopic images of female *I. ricinus*. (A–D) Ticks are shown with six legs in contact with the substrate while walking on a sloped gramineous leaf surface (A), horizontally on a resin replica of human female skin from the ventral forearm (B,C) and upside-down attached to glass (D). (E) Ventral detail of claws held apart: between them, the expanded, translucent pad and dorsal plates are visible. (F,G) Shiny blue areas in fluorescence light microscopy images demonstrate the presence of resilin in the tarsal–pretarsal articulation, in the lateral view of the pad and claw cuticle (F) and dorso-lateral view of the pretarsus with a partly unfolded pad (G). Arrowheads in B indicate the elastic tarsal–pretarsal articulation in contact with the substrate, while the pretarsus is held dorsally backwards. c, claw; e, expanded pad; f, folded pad; p, pad; t, tarsus; tp, tarsal–pretarsal articulation; u, unfolded pad.

The pad was composed of three lobes held together by dorsal plates. The surface of the pad was covered with 376.9±58.47 nm (*n*=14)-wide and 296.4±7.42 nm (*n*=5)-deep folds (folded condition). On

Fig. 3. Cryo-SEM micrographs of the pretarsus of *I. ricinus*. (A) The lateral view shows (1) paired curved, lunate, tapered claws, (2) sclerites and (3) extendable, folded pad. (B) Detail of cuticular folds on the ventral surface of the folded pad. (C) Ventral view of the pretarsus with an unfolded pad and spaced claws. (D,E) Ventral aspect of the folded pad (D) and dorsal view of the folded pad and tightly held claws (E). c, claw; d, dorsal plate; tp, tarsal–pretarsal articulation; p, pad; t, tarsus; v, ventro-lateral plate.

the ventral pad surface, centrally located folds were perpendicularly arranged; laterally located ones ran at an angle of 45 deg. Dorsally, folds were oriented transversely to the pad base.

The internal material of the pad was composed of a hierarchical network of fibres embedded in an amorphous matrix or lumen (Figs 4 and 5). Five distinct layers of fibre arrangement could be distinguished. (1) Densely packed nanofibres connected the pad to the 3 µm-thick scleral backing, the so-called dorsal plate, composed of cuticle layers which were crossed by large pore channels (Fig. 5A,E,F). (2) Single nanofibres were linked to fibre bundles, creating an 8 µm-thick and 39 µm-wide meshwork, which merged into larger, solid rope-shaped fibre bundles (Figs 4A and 5B). (3) The meshwork of 1.6±0.20 µm (*n*=10) thick bundles filled up a 50 µm-thick portion of the pad. Interspaces between bundles were 1.9±0.55 µm (*n*=20). (4) Ventrally, large fibre bundles diverged into 0.3±0.06 µm (*n*=10)-thick fibre bundles, which split into single, 65.5±17.17 nm (*n*=20)-thick nanofibres (Fig. 4B,D). (5) The 5 µm-thick fibre bundle-fibre layer was terminally covered with a 23.2±1.39 nm (*n*=20)-thick, folded membrane (epicuticle) (Figs 4C and 5A–D). The highly electron-dense, clear layer of epicuticle was interrupted by numerous, diffuse, permeable nanofolds, containing accumulated secretion (Fig. 5C,D). The thickness of the pad gradually increased in the distal direction, from about 22 to 96 µm. In the proximal half of the pad, rope-shaped and thinner fibre bundles were oriented perpendicularly to the scleral backing. In the distal half, they were aligned distally at an angle of 45 deg. Nanofibres were perpendicularly to the membrane and backing. Neither transversely running fibres nor pore channels were detected inside the pad.

The pad folded and unfolded similar to a fan at different degrees of opening, depending on the body posture, abiotic conditions and acting forces. Three conditions of the pad were observed: folded, unfolded and expanded (Figs 2 and 3; Movie 1). While folded, the pad was widely covered by dorsal and ventral plates, and the claws were held close together, parallel to each other (Figs 3E and 6A). We observed that in this condition, the entire pretarsus was frequently kept uplifted in the perfectly fitting cavity of its counterpart, the distal, dorsal tarsus (Fig. 2B). Walking horizontally without disturbance, pretarsi mostly remained in that position, and ticks used the soft tarsal–pretarsal articulation to contact the substrate.
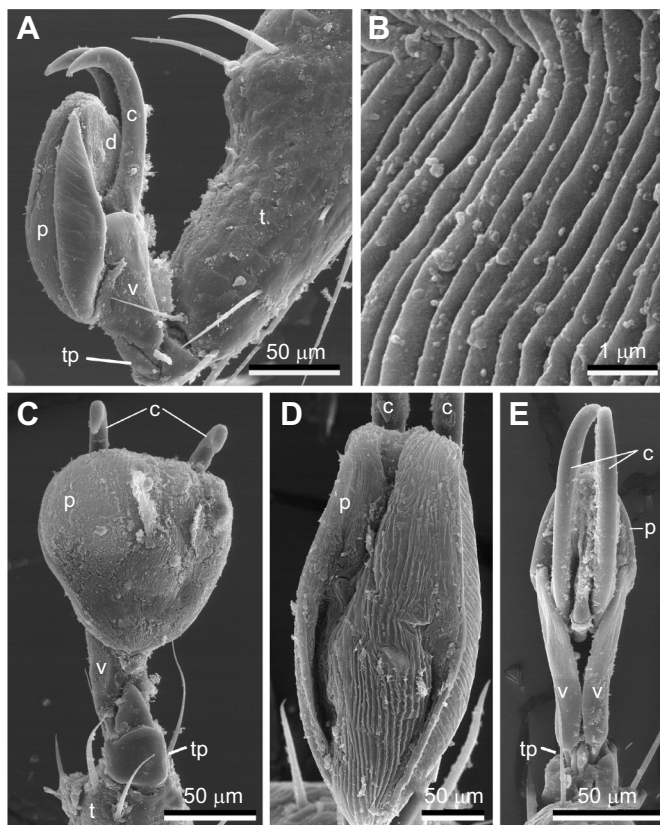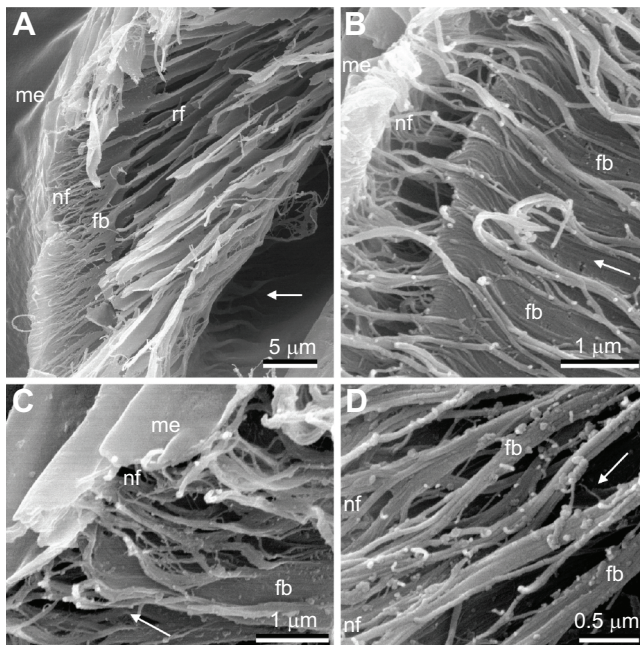
Fig. 4. Freeze fractures of the ixodid pretarsal pad (cryo-SEM). (A) Sagittal aspect of the internal hierarchical arrangement of backing rope-shaped fibre bundles, emerging smaller fibre bundles and nanofibres that split from these, covered with a membrane. (B) Transition zone between fibre bundles and nanofibres. (C) Detail of nanofibres covered with the membrane. (D) Detail of fibre bundles splitting into nanofibres. Arrows point ventrally. me, membrane; nf, nanofibre; fb, fibre bundle; rf, rope-shaped fibre bundles.

Adhesive pads were applied to the surface, unfolding them trapezoidally by V-shaped spreading of both dorsal plates and claws (Figs 2C,D,G and 6B). This posture was observed in, for example, ticks attached to human skin, where pads and claws frequently grasp the edge of skin microfolds (Fig. 3C). Human skin

generally provided a rather non-structured substrate for ticks' feet, because claws and pads matched only a small area of the plateau between microfolds, which appeared less irregular or slightly rough (Fig. 6A). In particular, on the ceiling or after a disturbance like vibration, ticks totally expanded their pads. They spread their claws apart until the claw tips almost faced each other, and the shape of the pad in contact became ovoid (first legs) or circular (Figs 3C and 6B). At the upside-down position on the glass ceiling, the contact area of the pad differed statistically between legs, sexes and the unfolded and expanded condition (Table S3). It was larger (1) in first legs than in the other legs, (2) in females than in males, and (3) under expansion. The fully expanded pad of (questing) forelegs created instant contact with the surface of a passing host.

After detachment, ticks left noticeable footprints, spanning an average triangular area of $48,368.0\pm443.42$ μm^2 ($n=5$, forelegs) and an ovoid area of 7547.5 ± 121.12 μm^2 ($n=3$, other legs) (Fig. 6C–E). They appeared thinner in the middle, surrounded by a meniscus of a few micrometres in diameter. However, the height of the meniscus and the layer could not be measured precisely. Interestingly, the inner fluid layer of a rather thin footprint was observed to be frozen over, while the meniscus was not (Fig. 6D,E). Solid particles were frequently observed in the fluid.

Attachment

In 34% of inversions, *I. ricinus* fell off the test surface (χ^2 analysis of contingency table, $\chi^2_{13,138}=113.5$, $P\leq0.001$; Fig. 7). Ticks attached significantly better to smooth surfaces than to rough ones ($\chi^2_{13,117}=1273.1$, $P\leq0.001$). The lowest frequencies of attachment were obtained on the resin surface, with an average roughness of $R_a=2.94$ μm, and on the silicone replica of skin with 54% and 48% failed trials, respectively. The strongest hold was observed on the native human female skin of the ventral forearm (90%), which was rougher than glass and the resin replica of glass, but was much softer and had a higher FSE than that of resin and silicone.
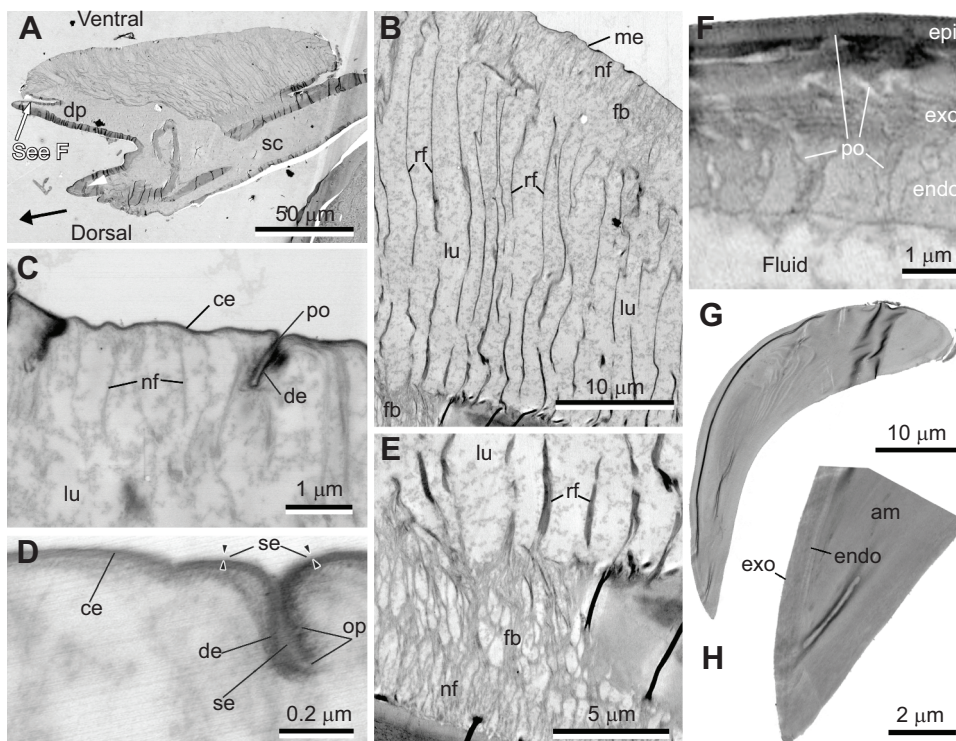

Fig. 5. TEM images of a sagittal section of the ixodid pretarsal pad and claw. (A) Pad and backing plate (sclerite). (B) A set of hierarchically arranged rope-shaped fibre bundles, smaller fibre bundles splitting into branching nanofibres, and an outer membrane. (C) Detail of nanofibres and membrane. (D) Detail of the membrane composed of a clear and diffuse epicuticle and covered with secretion. (E) The layer of fibres and branching nanofibres connecting the pad with the backing sclerites. (F) Detail of dorsal plate sclerite. (G) Aspect of the claw. (H) Detail of the distal claw. In A, the black arrow points distally; the white arrow indicates the site shown in detail in F; and the white arrowhead indicates the claw base and orientation of the claw tips. The black arrowheads in D show the superficial secretion. am, amorphous material; ce, clear epicuticle; de, diffuse epicuticle; dp, dorsal plate; epi, epicuticle; exo, exocuticle; endo, endocuticle; fb, fibre bundle; lu, lumen; me, membrane; nf, nanofibre; op, opening; po, pore; rf, rope-shaped fibre bundles; sc, sclerite; se, secretion.
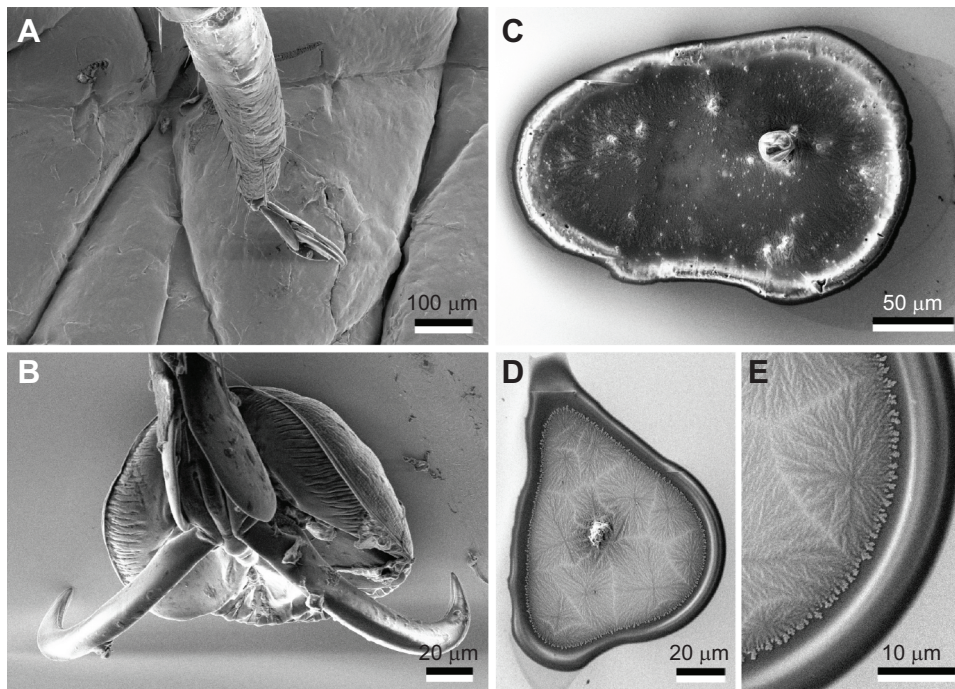
Fig. 6. Cryo-SEM micrographs of the pretarsus of *I. ricinus* attached to a substrate and 'footprints' following detachment. (A) Folded pad adhering to the resin replica of human ventral forearm skin. (B) Expanded pad in contact with a gold–palladium-sputtered smooth resin surface. (C–E) Residue of adhesion-mediating fluid left after detachment of the unfolded (C) and expanded pad (D,E). E is a detail of D, showing a distinct meniscus surrounding a thinner inner layer of fluid. The latter is covered by some frost mist although samples were sublimated.

The centrifugal force experiment resulted in significantly different friction forces and safety factors in *I. ricinus* males and females, independent of the FSE of the glass surface (normal glass versus silanised glass; Fig. 8). Maximum forces reached up to 5.9 and 6.3 mN in males and 7.9 and 8.5 mN in females on hydrophilic and hydrophobic glass, respectively. Thus, females generated 2.7 to 3.5 times higher forces than males on hydrophilic and hydrophobic glass, respectively. The mean body mass differed significantly between males (1.3 ± 0.70 mg) and females (1.8 ± 0.59 mg) (t-test,

t=2.8, P=0.008). Safety factors (friction force normalised by body weight) in females were up to 2.8 times higher than those of males (mean on hydrophobic glass 140.8 and 60.1, respectively). To withstand centrifugal forces, ticks kept their body very close to the surface, and held their legs at a wide angle to the body axis.

While walking horizontally (traction experiment), females produced 4.4 times higher maximum forces than when withstanding centrifugal forces on hydrophilic (normal) glass (9.2 ± 7.70 mN). Significantly lower forces were measured during traction on the
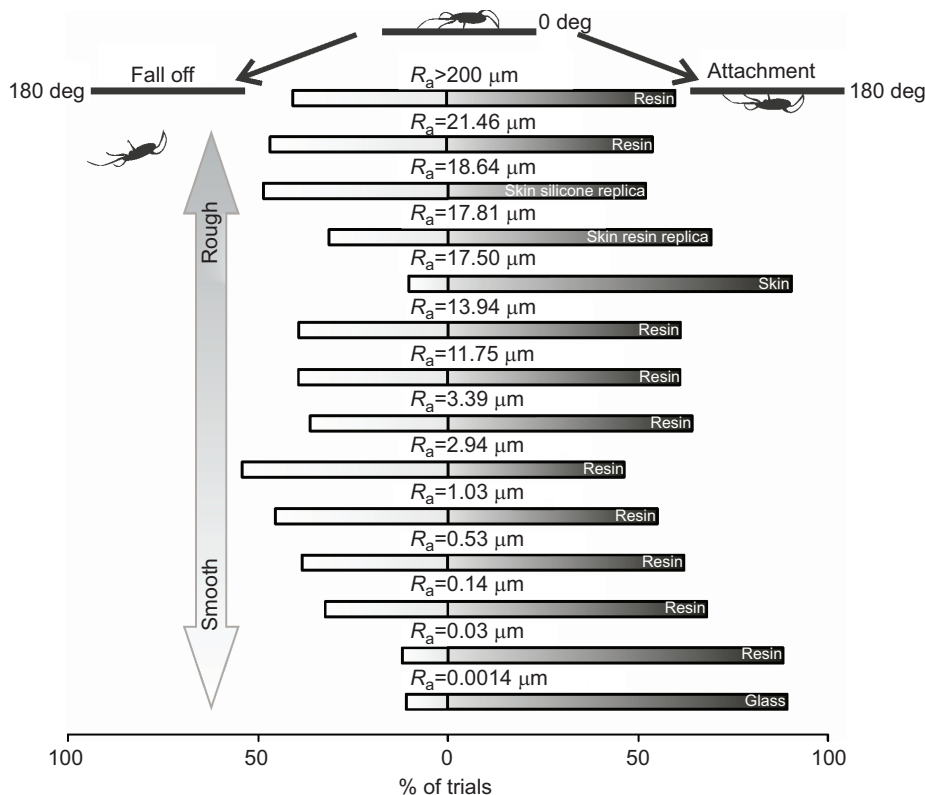

Fig. 7. Attachment ability of unfed female *I. ricinus* obtained in the inversion tests for various surface types. Attachment ability is shown as the frequency of attachment (percentage of trials) for the different substrates. The average roughness R_a (µm) is the average of the individual heights (asperities) and depths from the arithmetic mean elevation of the surface profile. Statistical differences (analysis of contingency tables) between frequencies of compared categories 'fall off' and 'attachment': $\chi^2_{13,138}$=113.5, $P \le 0.001$; between frequencies of compared surfaces: $\chi^2_{13,117}$=1273.1, $P \le 0.001$. The two characteristics that define the contingency table are significantly related ($P \le 0.001$).
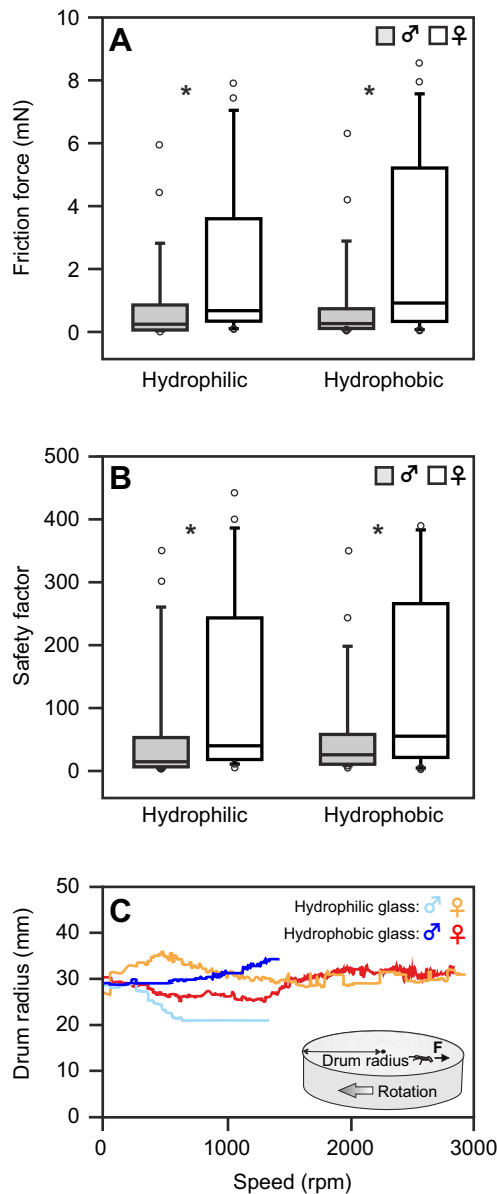
Fig. 8. Performance of *I. ricinus* obtained in the centrifugal force experiment. (A,B) Friction forces generated by unfed male and female *I. ricinus* (A) and their safety factors (B) on hydrophilic and hydrophobic glass. Contact angles of water were 42 and 108 deg, respectively (see Table S1). The ends of the boxes define the 25th and 75th percentiles, with a line at the median and error bars defining the 10th and 90th percentiles; circles are outliers. Asterisks indicate statistical differences between males and females according to Mann–Whitney rank sum test: $T=789$, $P=0.003$ for forces on hydrophilic glass; $T=772$, $P=0.009$ for forces on hydrophobic glass; $T=736$, $P=0.015$ for safety factors on hydrophilic glass; $T=742$, $P=0.044$ for safety factors on hydrophobic glass ($N_\male=25$, $N_\female=25$). No statistical differences in forces and safety factors between hydrophilic and hydrophobic glass were detected (force: $T=605$, $P=0.535$ in males, $T=625$, $P=0.816$ in females; safety factor: $T=591$, $P=0.372$ in males, $T=625$, $P=0.816$ in females). (C) Examples of sliding curves obtained in centrifugal force tests. The inset illustrates the experimental setup. **F**, force.

silicone replica of human skin (1.6±1.31 mN) (Fig. 9). Forces on native skin were significantly lower than those on glass; however, they did not differ statistically from forces on the Spurr resin replica of skin, although FSE distinctly varied between the surfaces. During the experiment, ticks were observed to apply their pretarsal pads and claws to the surfaces. They slightly raised the hind body, while the first
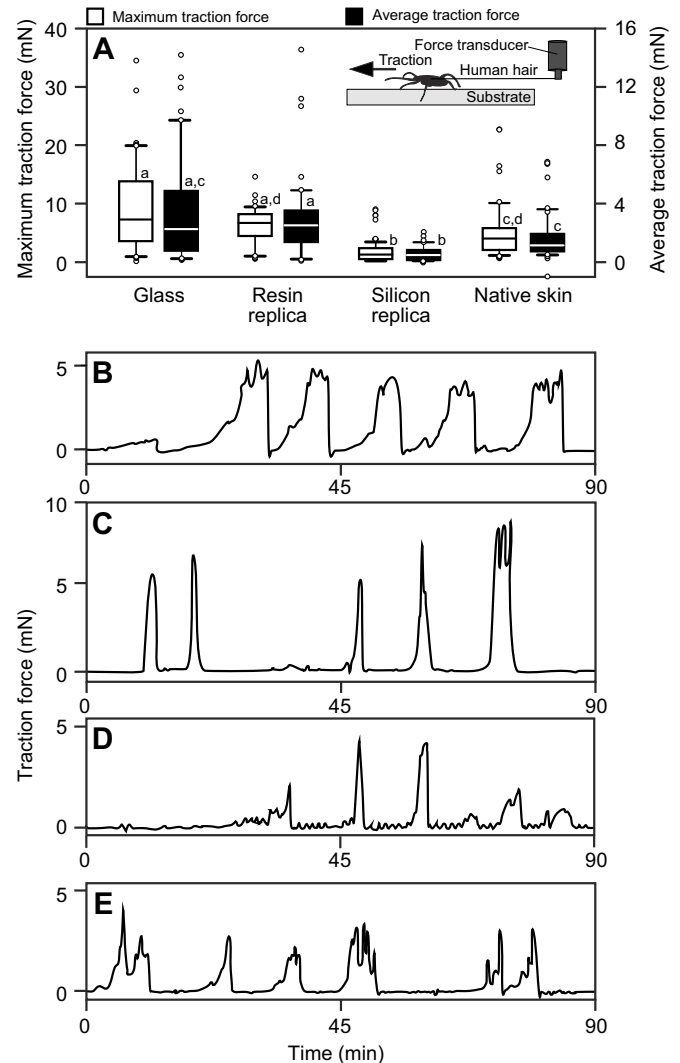

Fig. 9. Traction forces generated by unfed female *I. ricinus* on various substrates. (A) Box-and-whisker diagrams of maximum and average traction force for tick females on glass, native skin of human female ventral forearm and its resin and silicone replicas. Different letters indicate statistical differences in forces between surfaces for boxes of the same colour (Kruskal–Wallis one-way ANOVA on ranks followed by multiple comparison procedure Tukey test, $P<0.05$, maximum force obtained from peaks: $H_{3,48}=66.5$, $P\leq0.001$, average force over time obtained from the area under the curve: $H_{3,48}=58.2$, $P\leq0.001$). The ends of the boxes define the 25th and 75th percentiles, with a line at the median and error bars defining the 10th and 90th percentiles; circles are outliers. The inset illustrates the experimental setup. (B–D) Examples of force–time curves obtained from traction force measurements on the different substrates (B, glass; C, resin; D, silicone; E, skin).

and second legs were pulling forward. However, the bases of the third and fourth legs were kept perpendicular to the body axis by curving, the main portion of the legs was aligned forward and the pretarsi were kept distally inclined, capable of both pulling and pushing, depending on twisting. Mean body weight of the tested females was 1.7 ±0.38 mg, resulting in safety factors from 93 to 534 in the traction experiment on silicone and glass, respectively.

DISCUSSION
Soft and flexible, but tough: tarsal functional morphology

Ixodes ricinus exhibits an elaborate attachment system, comparable to the smooth attachment systems of hexapods according to Beutel

and Gorb (2001). Because of their elastically articulated segments, the legs appear to be flexible but strong, adaptable to flat, irregular and rod-shaped substrates. Unlike unidirectionally movable podomeres, the pretarsus seems to move in any direction at the soft tarsal–pretarsal articulation. The tarsal–pretarsal articulation appears membranous, compliant and possibly adhesive owing to the presence of soft elastic resilin (Fig. 2F,G). It is reminiscent of aphid attachment on smooth substrates, applying foldable, soft thickenings at the tibiotarsal joints while holding tarsi off the substrate (Lees and Hardie, 1988). Uplifted pretarsal structures, including the arolium, are also known in heelwalkers (Mantophasmatodea). They only use arolia when additional adhesion force is needed, in order to keep the adhesive surface away from debris and surface asperities that could contaminate or even damage the thin fragile surface of the arolium (Eberhard et al., 2009). Such a strategy must be also advantageous for ticks, considering their longevity and the less sclerotised acarid pretarsus (Alberti and Coons, 1999).

Claws of *I. ricinus* appeared translucent and resilin bearing (Fig. 2E–G). Resilin has previously been reported in the tarsi of several insect species (Gorb, 1996; Frazier et al., 1999; Federle et al., 2001; Niederegger and Gorb, 2003; Frantsevich and Gorb, 2004; Voigt et al., 2007; Michels et al., 2016). The specific protein is also a known component in the extensible alloscutal cuticle in *I. ricinus* females (Dillinger and Kesel, 2002; Andersen and Roepstorff, 2005). To our knowledge, this is the first confirmation of resilin in arthropod claws. However, its presence is expected in the claws of many more species and has probably been overlooked so far because of the melanisation of samples. As recently demonstrated for dragonfly wings, resilin is more evident in transparent veins using fluorescence microscopy, even though it is also detectable in the endocuticle of melanised veins by using sectioning methods (Appel et al., 2015).

Ixodid claws are expected to be highly elastic and adaptable as well as tough (Fig. 2C). In contrast to the trapezoid cross-section of reinforced claws of many other arthropods, the nearly circular ixodid claws seem to be a kind of bendable beam, also reflected by their high aspect ratio. Tick claws are distinctly longer (135 μm) than those of previously studied hexapods (e.g. 75 μm in mirid bugs and 96 μm in chrysomelid beetles; Voigt et al., 2007; D.V., unpublished data).

Claws in insects and oribatid mites are devices facilitating interlocking with structures in rough and filamentous terrains (Dai et al., 2002; Heethoff and Koerner, 2007; Voigt et al., 2007). The lunate curvature of the tick claw, fitting a circle of 55 μm diameter, suggests the ability to hook fibres such as plant trichomes and vertebrate epidermal hairs, spanning diameters of the micrometre to millimetre scale (Danforth and Trotter, 1922; Garn, 1951; Voigt et al., 2007; Kshirsagar et al., 2009). The elasticity of claws probably supports clasping of a broad range of fibre diameters by bending of the not completely rigid structure under load. Moreover, claws may operate as springs in a clinging tick, damping host movements and snapping back like a rubber band when separating forces act on the ectoparasite, keeping it attached to the substrate without any damage to either host or ectoparasite.

The contracted claw flexor muscle will cause pad unfolding and facilitate its contact to the substrate (Snodgrass, 1956; Federle et al., 2001; Frantsevich and Gorb, 2002, 2004; Federle and Endlein, 2004). Similar inflation/deflation behaviour has been reported from the smooth adhesive pads of insects such as Thysanoptera (Heming, 1971) and Hymenoptera (Baur and Gorb, 2001; Federle et al., 2001, 2002; Frantsevich and Gorb, 2002, 2004), and prenymphal whip

spiders and whip scorpions (Wolff et al., 2015a,b). However, the fan-like folding mechanism in pads of *I. ricinus* appears to be quite outstanding, allowing ticks to tune attachment forces not only by shearing but also by defining the contact area of the partially unfolded pad, depending on conditions/requirements (Fig. 10E–H). Actions are supported by several morphological features described in this paper: (1) distinct cuticular folds on the pad surface, (2) the presence of resilin inside the pad, and (3) the hollow bladder-like appearance of the pad reinforced with an internal fibrous structure (Fig. 10D). Previously, microstructural patterns have been reported from the surface of smooth adhesive pads of different insect taxa (Beutel and Gorb, 2001, 2006), playing a role in pad folding (Scholz et al., 2008) and prevention of aquaplaning (Gorb, 2007a). The pad microsculpture in *I. ricinus* is similar to patterns found in mecopteran and lepidopteran arolia (Beutel and Gorb, 2001; Al Bitar et al., 2009), and heteropteran (pseudo)pulvilli (Gorb and Gorb, 2004; Voigt et al., 2007). The fibrous anatomy and fibre bundle branching principle of ixodid pads resembles that of arolia in honeybees (Baur and Gorb, 2001), arolia in stick insects (Scholz et al., 2008; Bennemann et al., 2011; Labonte et al., 2014), prolegs in lepidopteran larvae (Hasenfuss, 1999) and euplantulae in grasshoppers (Kendall, 1970; Henning, 1974; Perez Goodwyn et al., 2006). Like ixodid pads, grasshopper euplantulae possess a distinct hierarchical arrangement of fibre layers, resulting in two levels of deformation when they contact the substratum (Gorb et al., 2000). Primary, deeper located, stiffer, rope-shaped fibre bundles probably keep the pad in shape, resisting tensile strength in the dorso-ventral direction. As no cross-links between fibres were observed in ticks, they are assumed to be deformable and to spread apart while unfolding the pad. Because of their distal alignment, they may prevent the pad from damage under shear stress during sliding and under tensile stress during pulling off. The dimensions of tick pad layers and fibres correspond to the thin membranous superficial layer and loosely packed fibres in the euplantulae of bush crickets, which have been reported to be much softer, flexible and more adhesive than pads in migratory locusts, containing densely arranged and tightly interconnected filaments (Perez Goodwyn et al., 2006).

While attaching and climbing on rod-shaped substrates such as plant stems or bundles of host hairs (Fig. 10C), ticks clamp structures between their feet. Sandwich-like fibrillar materials and foam-like rubbers as found in tarsal pads, terminated with a thin film have turned out to be the most promising, inspiring materials for gripping devices for climbing robots (Voigt et al., 2012). Because of their compliance, soft pads enhance the contact area with the substrate as found for the arolium of some cockroaches (Arnold, 1974), increasing adhesion as a result of the action of intermolecular forces between the pad and substrate (Kendall, 2001). This effect is supported by tarsal secretion, indicated by the presence of clear footprints after detachment of a tick's pad, which is optically similar to the secretion found at smooth adhesive organs of other insects, e.g. cockroaches (Roth and Willis, 1952), orthopterans (Jiao et al., 2000; Vötsch et al., 2002), stick insects (Drechsler and Federle, 2006; Scholz et al., 2008), aphids (Lees and Hardie, 1988; Dixon et al., 1990), true bugs (Edwards and Tarkanian, 1970; Hasenfuss, 1977a,b, 1978; Ghazi-Bayat and Hasenfuss, 1980a,b, 1981) and hymenopterans (Federle et al., 2001, 2002). It has previously been suggested that the fluid is transported from the epidermis to the surface of the epicuticle through thin canals (cockroaches: Arnold, 1974; locust: Schwarz and Gorb, 2003), although other authors could not detect these pores in the cuticle of the stick insect arolium (Scholz et al., 2008). Inside pads of *I. ricinus*, we found neither
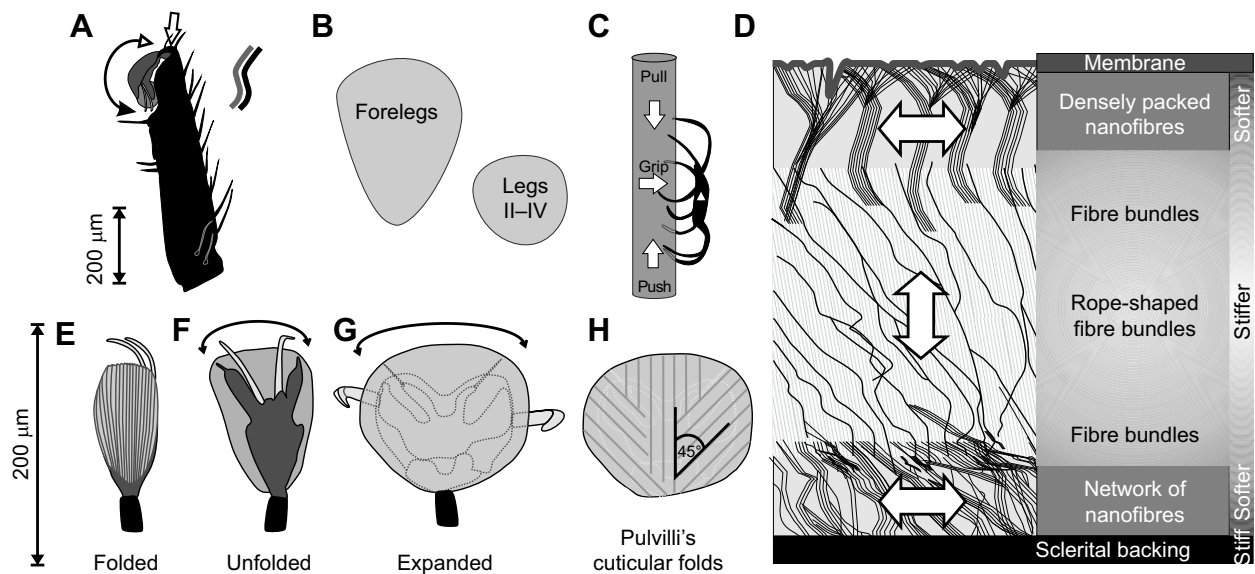
Fig. 10. Schematic diagram of tarsal states. (A) The tarsus bears a distal articulation (arrow), flexibly coupling to the pretarsus; the latter is folded backwards (double arrow) perfectly fitting into the dorsal outline of its counterpart, the distal tarsal segment (represented by the sigmoid double lines in the inset). (B) Differences in pad dimension and shape between the forelegs and other legs. (C) The tick walking upwards on a rod-shaped substrate, properly attached by the multidirectional support of both pretarsal attachment and posture of four pairs of legs: the forelegs pulling, the hindlegs pushing, and the second and third pair of legs gripping the substrate. The white arrowhead points to the anterior direction of the tick's body. (D) Diagram illustrating the internal organisation of the ixodid pretarsal pad (sagittal view), appearing like a sandwich of fine, flexible, adaptable fibres, with a layer of stiffer rope-shaped fibre bundles in between. Ventrally and dorsally, large rope-shaped fibre bundles branch into smaller fibre bundles. The latter further split into nanofibres, which are ventrally covered by a thin epicuticular membrane, and dorsally connect the pad to the pretarsal sclerite. Arrows indicate the hypothetical direction of tension acting inside the pad. (E–H) Various states of the foldable pad, ventrally (E,G,H) and dorsally (F). Double arrows indicate the direction of folding–unfolding motion.

pores nor channels. On the pad surface, permeable nanofolds interrupt the epicuticle. They may act as a kind of specific pore, by squeezing the adhesive secretion during pad contact formation. A tarsal gland has previously been detected, whose duct terminates in the pad. Its role in the functioning of the pad as an adhesive organ by the production of non-proteinaceous, lipoid secretion was proposed (Baker, 1997; Leonovich, 2010). As the lateral plates surrounding the pad are equipped with many pore canals (Baker, 1997; present study), one may further suggest that fluid is secreted there and runs over the pad via cuticular folds which have previously been assumed to be a fluid transporting system in pulvilli of representatives of the order Heteroptera (Hasenfuss, 1977a; Ghazi-Bayat and Hasenfuss, 1980a,b, 1981). Thus, rapid spreading, drainage of pad secretion, control of secretion thickness and prevention of aquaplaning may be simultaneously realised (Ohler, 1995; Scherge and Gorb, 2001; Barnes, 2007; Gorb, 2007a; Scholz et al., 2008; Varenberg and Gorb, 2009; Barnes et al., 2013). Additionally, the microsculpture of smooth pads can prevent stick–slip motion on smooth substrata (Varenberg and Gorb, 2009), and may provide a better grip on non-smooth substrata (Drechsler and Federle, 2006). Although footprints of ticks appear much bulkier than those of other arthropods, we suggest a similar biphasic composition of the fluid (lipid nanodroplets dispersed in an aqueous liquid) to that reported for locusts (Vötsch et al., 2002). Thus, the frost cover in Fig. 6D,E could be explained as being caused by the aqueous portion of the fluid, surrounded by a lipoid meniscus. In addition to the increase of adhesion by capillary effects, pad cleaning might be another function of the fluid because it may rinse off contaminating particles, which are frequently observed inside the footprints.

Considering the above discussed properties, tarsal pads of *I. ricinus* seem to be most similar to hymenopteran arolia; however, they do not perfectly match the definition of either arolia or pulvilli.

Attachment ability

Tick attachment was reduced on inverted rough resin substrates, especially on those with average roughness values of R_a=1.0, 2.9 and 21.46 μm, while it was strongest on native skin (R_a=17.5 μm), smooth resin (R_a=0.03 μm) and glass (R_a=0.001 μm). Although we just evaluated the proportion of animals that remained attached after substrate inversion and did not measure forces during inversion, our observations roughly correspond to previous reports, where roughness values of 0.3, 1.0 and 3.0 μm have been stated to decrease friction forces in insect and spider attachment pads (Peressadko and Gorb, 2004; Voigt et al., 2008; Al Bitar et al., 2010; Wolff and Gorb, 2012). This effect is thought to be due to the decrease of contact area between adhesive pads and substrates and to the failure of claw interlocking. Although single adhesive pads of *I. ricinus* cover many irregularities of rough surfaces, they cannot adjust sufficiently to the substrate profile of some critical roughness values, probably because of limited compliance. As arthropod claws can interlock only with substrate projections, which are significantly larger than the claw tip diameter, ticks are unable to grip minute surface irregularities smaller than 1.2 μm, and slip off such a substrate (Dai et al., 2002). Interestingly, a large portion of ticks fell off resin surfaces rougher than 1.2 μm. Here, flexible claws meet a flat, stiff substrate and cannot reliably interlock. In contrast, on soft native skin, 90% of ticks remained attached after inversion. A similar portion of ticks successfully attached to smooth surfaces, to which smooth pads are specialised as previously demonstrated in stick insects (Bußhardt et al., 2012). This fact may be another explanation for the strong attachment on human skin as an unfolded/expanded pretarsal pad in tick meets the relatively smooth plateau between skin microfolds (Figs 2B,C and 6A).

Friction measured in the centrifuge experiment is the resistance force of the body mass to the sum of centrifugal and tangential forces acting on the animal along the substrate plane (Gorb et al.,

2001). Females generated much higher forces than males. However, no significant differences in friction forces and safety factors were found between hydrophilic and hydrophobic glass within one sex. This effect may be attributed to the assumed biphasic nature of the adhesive fluid having ubiquitous wetting properties. Safety factors of female *I. ricinus* (mean 141) were notably higher than those of males (mean 60). Previous data obtained under similar experimental conditions showed an opposite trend in tortricid moths on glass (males: 19, females: 13; Al Bitar et al., 2009) and in chrysomelid beetles on smooth resin (dock leaf beetle males: 100, females: 50; Zurek et al., 2016; Colorado potato beetle males: 71, females: 60; Voigt et al., 2008). While the better performance of males has been explained by sexual dimorphism in shape of tarsal adhesive setae in leaf beetles, such a dimorphism was not observed in moths and, thus, differences in material properties of smooth adhesive pads were assumed to be the reason for this difference. In ticks, female adhesive pads are distinctly larger than male ones. Higher safety factors in female *I. ricinus* correspond well to the 135 times increase of female body weight while feeding and when replete (Oliver, 1989; Dautel, 1995; Uspensky et al., 1999). Males do not rely on higher safety factors because they take up a negligible amount of blood without a significant increase of body weight (Liebisch and Liebisch, 2003). However, their safety factor of 60 should not be underestimated. The comparatively high safety factors of *I. ricinus* provide clear advantages in terms of resistance to regular exogenous impact, especially movements of the host at any velocity (Lees, 1948).

Supporting information about pad performance comes from lateral tenacity (shear stress), which is determined as friction force divided by the overall area of all pads. Assuming that a tick has all legs, i.e. eight pads in contact, standing on the horizontal centrifugal drum surface, the maximum lateral tenacity on glass may be roughly estimated as $0.02\,\mu N\,\mu m^{-2}$ (female) and $0.008\,\mu N\,\mu m^{-2}$ (male). Compared with that of female ticks, tenacity is 10 times higher in arolia of adult tortricid moths ($0.2\,\mu N\,\mu m^{-2}$; Al Bitar et al., 2009), 5 times higher in pulvilli of adult coreid bugs ($0.1\,\mu N\,\mu m^{-2}$; Gorb and Gorb, 2004), but 3 times lower in adhesive pads in sawfly larvae ($0.006\,\mu N\,\mu m^{-2}$; Voigt and Gorb, 2012). Similar to fast movements of arolia in Mantophasmatodea (Eberhard et al., 2009), tick forelegs pads can suddenly be brought in contact with and instantly adhere to the host surface, facilitating first access and attachment to the host. By rough calculation, a single expanded pad on a female tick's foreleg generates force roughly corresponding to 31 times female body weight. This capability is sufficient for initial attachment of the forelegs to vertebrate hosts during transition from banker plants. However, one has to keep in mind that a single leg in contact commonly generates a lower force when compared with the contribution of legs acting together in concert with each other (Wohlfart et al., 2014).

The large scattering of values is noteworthy (0–8 and 0–400 in forces and safety factors, respectively). High standard deviations for ticks have previously been related to the large individual variability in bionomic studies (Dautel, 1995). However, all individuals of *I. ricinus* in our study were collected from a limited area, probably belonging to the same population, appearing to be active and fit. The range of body weight did not reflect the scattering of measured force values. We suggest further factors influence the attachment ability. For example, highly sensitive ticks commonly undergo a thanatosis after sudden disturbances, folding the legs ventrally and closely to the body, maintaining an immobile condition for a while (Babos, 1964). This could have happened in several individuals during the present experiment, resulting in low measured force values. Another

reason could be the fluid-driven dynamics of the foldable adhesive pad, which is related to inner fluid pressure and muscle movements and thus represents a rather dynamic system, which may interfere with the rotating situation on the centrifuge drum. Similar assumptions have been published for soft-bodied, short-legged sawfly larvae where attachment devices are mainly hydrostatically controlled, resulting in a limited control of contact formation and breakage and therefore adhesion and friction (Voigt and Gorb, 2012).

The finding of highest traction of ticks on glass supports the hypothesis that smooth pads are specialised for smooth, flat substrates (Bußhardt et al., 2012). Shearing of tick pads on glass resulted in rapidly increasing force–time curves, usually followed by a plateau before forces returned to zero (Fig. 9B). In contrast, while tracking on resin replicas of skin, there were strong pulls but no plateaus, with forces returning quickly to the baseline (Fig. 9C). Possibly, elastic claws and pads behave like rubber and flip off the rigid substrate above a certain applied pulling force. This could also explain the higher fall-off proportion on resin substrates in the inversion experiment. In comparison, traction (force–time) curve peaks on native skin were lower, but they were observed frequently on small relatively smooth plateaus of the skin microstructure as a result of pad shear movements (Fig. 9E). Low-level undulations, obtained on the silicone replica of skin, resemble stick–slip events probably during sliding of pads and claws (Fig. 9D). Ticks performed poorly, in terms of both attachment and locomotion, on the low surface energy silicone surface in comparison to their good performance on glass. Interestingly, the mean safety factor obtained on glass was higher in traction (534) than in centrifugal force experiments (441), which may be an additional hint for the significance of pretarsal dynamics in tick attachment.

The tick–skin interface
When tick tarsal pads attach to the human skin, two multilayered composite materials meet each other. Both are soft biomaterials with a complex anatomical structure, characterised by viscoelastic material behaviour. As friction behaviour strongly depends on the contact conditions at the triobinterface, it is influenced by physical and physiological skin conditions (hydration state, sebum level), contact parameters (normal load), sliding velocity, age, sex, ethnicity and anatomical region of the skin (Derler and Gerhardt, 2012). Like skin, tick pretarsal pads probably rely on the displacement of interstitial fluid through a fibrous network by the stretching and compression of fibres. As a result, pads adapt to a wide range of skin surface topography, which depends on the body region and is characterised by ridges or furrows that delimit polygonal areas of variable size. Typical roughness values of skin range from R_a=10 to 30 μm all over the body. Hence, a limited insight is given by our study using the female volar forearm (R_a=18 μm) as a sample substrate. One may expect different interfacial effects between tick tarsi and human skin at various sites of the body, resulting in different attachment ability.

Considering the present results, we suggest that claws operate as anchors and levers, while adhesive pads mainly contribute to tick attachment on vertebrate hosts, which provide suitable contact points for the 100–140 μm-wide adhesive pads of ticks by numerous hair-free sites between the 200 to 25,000 hairs of 25–160 μm width per cm^2 (Dathe, 1986; Kshirsagar et al., 2009).

The significance of host pelage related to ectoparasites has been controversially discussed. For bed bugs, which prefer hairless sites, the layer of fine hair covering the human body at a relatively high follicular density increased search time and enhanced the detection of

parasites (Reinhardt and Siva-Jothy, 2007; Dean and Siva-Jothy, 2012). In contrast, hairs have been supposed to offer hiding place and habitat for ticks. In that context, the evolution of nakedness in humans has been explained, amongst others, by adaptation against ectoparasites (Rantala, 1999, 2007). Knowing ticks' preference for non-structured surfaces, the loss of functional body hair in humans seems to be more advantageous in terms of prevention of hyperthermia than with regard to ticks, as previously suggested by alternative hypotheses (Schwartz and Rosenblum, 1981; Wheeler, 1985).

Conclusions and outlook

Podomeres and pretarsi of *I. ricinus* are flexible as a result of both the presence of the elastic protein resilin and specific morphology. The arrangement of segments and inner fibres within adhesive pads lets them act multidirectionally in shearing and in pull-off direction. The multi-layered adhesive pad, being compliant and adaptable to the substrate profile, resists substantial tensile and shear forces while gripping/clamping, pulling and pushing. The fan-like folding mechanism of the pads allows their application at different degrees of folding which results in fine tuning of contact areas and, consequently, attachment forces. A large amount of adhesion-mediating fluid provides some self-cleaning of the pad as well as substrate wetting and thus access of ticks to surfaces having different FSE. Additionally, surface asperities and irregularities may be filled and smoothed by the fluid. Accordingly, ticks are able to attach to a broad range of various natural substrates, including sebum-covered skin, pelage of hosts and the waxy and pubescent surface of plants. However, the strongest attachment forces were generated on glass and human skin. On silicone skin replicas, ticks attached less well, which may be an interesting hint for tick control strategies and future studies.

References
Al Bitar, L., Voigt, D., Zebitz, C. P. W. and Gorb, S. N. (2009). Tarsal morphology and attachment ability to the codling moth *Cydia pomonella* L. (Lepidoptera, Tortricidae) to smooth surfaces. *J. Insect Physiol.* **55**, 1029-1038.
Al Bitar, L., Voigt, D., Zebitz, C. P. W. and Gorb, S. N. (2010). Attachment ability of the codling moth *Cydia pomonella* L. to rough substrates. *J. Insect Physiol.* **56**, 1966-1972.
Alberti, G. and Coons, L. B. (1999). Acari - Mites. In *Microscopic Anatomy of Invertebrates*, Vol. 8c (ed. F. W. Harrison and F. W. Foelix), pp. 515-1215. New York: Wiley-Liss.
Alekseev, A. N. and Dubinina, H. V. (2006). Evidence that tick attachment to the human skin isn't random. *Acarina* **14**, 203-208.

Alekseev, A. N., Jensen, P. M., Dubinina, H. V., Smirnova, L. A., Makrouchina, N. A. and Zharkov, S. D. (2000). Peculiarities of behaviour of taiga (*Ixodes persulcatus*) and sheep (*Ixodes ricinus*) ticks (Acarina: Ixodidae) determined by different methods. *Folia Parasitologica* **47**, 147-153.
Allan, S. A. (2010). Chemical ecology of tick-host interactions. In *Ecology and Control of Vector-borne Diseases. Vol. 2: Olfaction in Vector-host Interactions* (ed. W. Takken and B. G. J. Knols), pp. 327-348. Wageningen: Wageningen Academic Publishers.
Andersen, S. O. and Roepstorff, P. (2005). The extensible alloscutal cuticle of the tick, *Ixodes ricinus. Insect Biochem. Mol. Biol.* **35**, 1181-1188.
Andersen, S. O. and Weis-Fogh, T. (1964). Resilin. A rubber-like protein in arthropod cuticle. *Adv. Insect Physiol.* **2**, 1-65.
Appel, E., Heepe, L., Lin, C.-P. and Gorb, S. N. (2015). Ultrastructure of dragonfly wing veins: composite structure of fibrous material supplemented by resilin. *J. Anat.* **227**, 561-582.
Arnold, J. W. (1974). Adaptive features on the tarsi of cockroaches (Insecta: Dictyoptera). *Int. J. Insect Morphol. Embryol.* **3**, 317-334.
Arthur, D. R. (1945). Hatching of the egg of *Ixodes ricinus* L. *Nature* **156**, 538.
Babos, S. (1964). *Die Zeckenfauna Mitteleuropas*. Budapest: Akadémiai Kiadó, Druckerei der Ungarischen Akademie der Wissenschaften.
Baker, G. T. (1997). The pulvillus: cuticular structure and function (Acarina: Ixodida). *J. Acarol. Soc. Jpn.* **6**, 25-31.
Barnes, W. J. P. (2007). Functional morphology and design constraints of smooth adhesive pads. *MRS Bull.* **32**, 479-485.
Barnes, W. J. P., Baum, M., Peisker, H. and Gorb, S. N. (2013). Comparative Cryo-SEM and AFM studies of hylid and rhacophorid tree frog toe pads. *J. Morphol.* **274**, 1384-1396.
Baur, F. and Gorb, S. N. (2001). How the bee releases its leg attachment devices. In *Technische Biologie und Bionik. 5. Bionik-Kongress, Dessau 2000* (ed. A. Wisser and W. Nachtigall), pp. 295-297. Stuttgart, Jena, Lübeck, Ulm: Gustav Fischer Verlag.
Bennemann, M., Scholz, I. and Baumgartner, W. (2011). Functional morphology of the adhesive organs of stick insects. *Proc. SPIE* **7975**, 79751A-1.
Beutel, R. G. and Gorb, S. N. (2001). Ultrastructure of attachment specializations of hexapods (Arthropoda): evolutionary patterns inferred from a revised ordinal phylogeny. *J. Zool. Syst. Evol. Res.* **39**, 177-207.
Beutel, R. G. and Gorb, S. N. (2006). A revised interpretation of the evolution of attachment structures in Hexapoda with special emphasis on Mantophasmatodea. *Arthropod Syst. Phyl.* **64**, 3-25.
Buczek, A. and Bartosik, K. (2006). Interakcje w ukladzie kleszcz-zywiciel. *Przegl. Epidemiol.* **60**, 28-33.
Buczek, A., Olszewski, T., Andrearczyk, A. and Zwolinski, I. J. (2004). Budowa stop kleszczy (Acari: Ixodida) – modyfikacje zwiazane z cyklem zyciowym, behawiorem i siedliskiem. *Wiad. Parazytol.* **50**, 285-294.
Bußhardt, P., Wolf, H. and Gorb, S. N. (2012). Adhesive and frictional properties of tarsal attachment pads in two species of stick insects (Phasmatodea) with smooth and nubby euplantulae. *Zoology* **115**, 135-141.
Cheng, T. C. (1973). *General Parasitology*. New York: Academic Press.
Coons, L. B. and Alberti, G. (1999). Acari - Ticks. In *Microscopic Anatomy of Invertebrates*, Vol. 8b (ed. F. W. Harrison), pp. 267-514. New York: Wiley–Liss, Inc.
Crooks, E. and Randolph, S. E. (2006). Walking by *Ixodes ricinus* ticks: intrinsic and extrinsic factors determine the attraction of moisture or host odour. *J. Exp. Biol.* **209**, 2138-2142.
Dai, Z., Gorb, S. N. and Schwarz, U. (2002). Roughness-dependent friction force of the tarsal claw system in the beetle *Pachnoda marginata* (Coleoptera, Scarabaeidae). *J. Exp. Biol.* **205**, 2479-2488.
Danforth, C. H. and Trotter, M. (1922). The distribution of body hair in white subjects. *Am. J. Physiol. Anthropol.* **5**, 259-265.
Dathe, H. (1986). *Pelztieratlas*. 323pp. Jena: Gustav-Fischer-Verlag.
Dautel, H. (1995). Untersuchungen zum Lebenszyklus und zur Kältebiologie von Zecken (Acari: Ixodoidea) unter besonderer Berücksichtigung der Taubenzecke, *Argas reflexus* und des gemeinen Holzbocks, *Ixodes ricinus*. PhD thesis, Freie Universität Berlin.
Dean, I. and Siva-Jothy, M. T. (2012). Human fine body hair enhances ectoparasite detection. *Biol. Lett.* **8**, 358-361.
Derler, S. and Gerhardt, L.-C. (2012). Tribology of skin: review and analysis of experimental results for the friction coefficient of human skin. *Tribol. Lett.* **45**, 1-27.
Dillinger, S. C. G. and Kesel, A. B. (2002). Changes in the structure of the cuticle of *Ixodes ricinus* L. 1758 (Acari, Ixodidae) during feeding. *Arthr. Struct. Dev.* **31**, 95-101.
Dixon, A. F. G., Croghan, P. C. and Gowing, R. P. (1990). The mechanism by which aphids adhere to smooth surfaces. *J. Exp. Biol.* **152**, 243-253.
Drechsler, P. and Federle, W. (2006). Biomechanics of smooth adhesive pads in insects: influence of tarsal secretion on attachment performance. *J. Comp. Physiol. A* **192**, 1213-1222.
Eberhard, M. J. B., Pass, G., Picker, M. D., Beutel, R., Predel, R. and Gorb, S. N. (2009). Structure and function of the arolium of Mantophasmatodea (Insecta). *J. Morphol.* **270**, 1247-1261.

Edwards, J. S. and Tarkanian, M. (1970). The adhesive pads of Heteroptera: a re-examination. *Proc. R. Ent. Soc. Lond. A* **45**, 1-5.

Enigk, K. (1953). *Zur Biologie der Zecken*. Hamburg: Titschack.

Falke, H. (1931). Beiträge zur Lebensgeschichte und zur postembryonalen Entwicklung von *Ixodes ricinus* L. *Ztschr. Morphol. Ökol. Tiere* **21**, 567-607.

Federle, W. and Endlein, T. (2004). Locomotion and adhesion: dynamic control of adhesive surface contact in ants. *Arthr. Str. Dev.* **33**, 67-75.

Federle, W., Brainerd, E. L., McMahon, T. A. and Hölldobler, B. (2001). Biomechanics of the movable pretarsal adhesive organ in ants and bees. *Proc. Natl. Acad. Sci. USA* **98**, 6215-6220.

Federle, W., Riehle, M., Curtis, A. S. G. and Full, R. J. (2002). An integrative study of insect adhesion: mechanics and wet adhesion of pretarsal pads in ants. *Integr. Comp. Biol.* **42**, 1100-1106.

Francischetti, M. B., Sá-Nunes, A., Mans, B. J., Santos, I. M. and Ribeiro, J. M. C. (2010). The role of saliva in tick feeding. *Front. Biosci.* **14**, 2051-2088.

Frantsevich, L. and Gorb, S. (2002). Arcus as a tensegrity structure in the arolium of wasps (Hymenoptera: Vespidae). *Zoology* **105**, 225-237.

Frantsevich, L. and Gorb, S. (2004). Structure and mechanics of the tarsal chain in the hornet, *Vespa crabro* (Hymenoptera: Vespidae): implications on the attachment mechanism. *Arthropod. Struct. Dev.* **33**, 77-89.

Frazier, S. F., Larsen, G. S., Neff, D., Quimby, L., Carney, M., DiCaprio, R. A. and Zill, S. N. (1999). Elasticity and movements of the cockroach tarsus in walking. *J. Comp. Physiol. A* **185**, 157-172.

Garn, S. M. (1951). Types and distribution of the hair in man. *Ann. N. Y. Acad. Sci.* **53**, 498-507.

Ghazi-Bayat, A. and Hasenfuss, I. (1980a). Die Oberflächenstrukturen des Prätarsus von *Elasmucha ferrugata* (Fabricius) (Acanthosomatidae Heteroptera). *Zool. Anz.* **205**, 76-80.

Ghazi-Bayat, A. and Hasenfuss, I. (1980b). Zur Herkunft der Adhäsionsflüssigkeit der tarsalen Haftlappen bei den Pentatomidae (Heteroptera). *Zool. Anz.* **204**, 13-18.

Ghazi-Bayat, A. and Hasenfuss, I. (1981). Über den Transportweg der Haftflüssigkeit der Pulvilli bei *Coptosoma scutellatum* (Geoffr.) (Plataspididae, Heteroptera). *Nachrichtenbl. Bayer. Entomol.* **30**, 5-8.

Gorb, S. N. (1996). Design of insect unguitractor apparatus. *J. Morphol.* **230**, 219-230.

Gorb, S. N. (1999). Serial elastic elements in the damselfly wing: mobile vein joints contain resilin. *Naturwiss.* **86**, 552-555.

Gorb, S. N. (2006). Fly microdroplets viewed big: a cryo-SEM approach. *Microsc. Today* **14**, 38-39.

Gorb, S. N. (2007a). Smooth attachment devices in insects: functional morphology and biomechanics. *Adv. Ins. Physiol.* **34**, 81-115.

Gorb, S. N. (2007b). Visualisation of native surfaces by two-step molding. *Microsc. Today* **15**, 44-46.

Gorb, S. N. and Gorb, E. V. (2004). Ontogenesis of the attachment ability in the bug *Coreus marginatus* (Heteroptera, Insecta). *J. Exp. Biol.* **207**, 2917-2924.

Gorb, S. N., Jiao, Y. and Scherge, M. (2000). Ultrastructural architecture and mechanical properties of attachment pads in *Tettigonia viridissima* (Orthoptera, Tettigoniidae). *J. Comp. Physiol. A* **186**, 821-831.

Gorb, S., Gorb, E. and Kastner, V. (2001). Scale effects on the attachment pads and friction forces in Syrphid flies (Diptera, Syrphidae). *J. Exp. Biol.* **204**, 1421-1431.

Gorb, E., Kastner, V., Peressadko, A., Arzt, E., Gaume, L., Rowe, N. and Gorb, S. (2004). Structure and properties of the glandular surface in the digestive zone of the pitcher in the carnivorous plant *Nepenthes ventrata* and its role in insect trapping and retention. *J. Exp. Biol.* **207**, 2974-2963.

Gorb, S. N., Schuppert, J., Walther, P. and Schwarz, H. (2012). Contact behaviour of setal tips in the hairy attachment system of the fly *Calliphora vicina* (Diptera, Calliphoridae): a cryo-SEM approach. *Zoology* **115**, 142-150.

Grenacher, S., Kröber, T., Guerin, P. M. and Vlimant, M. (2001). Behavioural and chemoreceptor cell responses of the tick, *Ixodes ricinus*, to its own faeces and faecal constituents. *Exp. Appl. Acarol.* **25**, 641-660.

Hackman, R. H. and Filshie, B. K. (1982). The tick cuticle. In *The Physiology of Ticks* (ed. F. D. Obenchain and R. Galun), pp. 1-42. Oxford: Pergamon Press.

Hasenfuss, I. (1977a). Die Herkunft der Adhäsionsflüssigkeit bei Insekten. *Zoomorphologie* **87**, 51-64.

Hasenfuss, I. (1977b). Woher stammt die Adhäsionsflüssigkeit, die bei Insekten ein Haften an glatten Flächen ermöglicht? *Verh. Deutsch. Zool. Gesell.* **277**, 277-1277.

Hasenfuss, I. (1978). Über das Haften von Insekten an glatten Flächen – Herkunft der Adhäsionsflüssigkeit. *Zool. Jb. Anat.* **99**, 115-116.

Hasenfuss, I. (1999). The adhesive devices in larvae of Lepidoptera (Insecta, Pterygota). *Zoomorphology* **119**, 143-162.

Healy, J. A. E. and Bourke, P. (2008). Aggregation in the tick *Ixodes ricinus* (Acari: Ixodidae): use and reuse of questing vantage points. *J. Med. Entomol.* **45**, 222-228.

Heethoff, M. and Koerner, L. (2007). Small but powerful: the oribatid mite *Archegozetes longisetosus* Aoki (Acari, Oribatida) produces disproportionately high forces. *J. Exp. Biol.* **210**, 3036-3042.

Heinze, D. M., Carmical, J. R., Aronson, J. F. and Thangamani, S. (2012). Early immunologic events at the tick-host interface. *PLoS ONE* **7**, e47301, 1-11.

Heming, B. S. (1971). Functional morphology of the thysanopteran pretarsus. *Can. J. Zool.* **49**, 91-108.

Henning, B. (1974). Morphologie und Histologie der Tarsen von *Tettigonia viridissima* L. (Orthoptera, Ensifera). *Z. Morphol. Tiere* **79**, 323-342.

Igarashi, T., Nishino, K. and Nayar, S. K. (2005). The appearance of human skin: a survey. *Found. Trends Comput. Graphics Vision* **3**, 1-95.

Jiao, Y., Gorb, S. N. and Scherge, M. (2000). Adhesion measured on the attachment pads of *Tettigonia viridissima* (Orthoptera, Insecta). *J. Exp. Biol.* **203**, 1887-1895.

Kemp, D. H., Stone, B. F. and Binnington, K. C. (1982). Tick attachment and feeding: role of the mouthparts, feeding apparatus, salivary gland secretions and the host response. In *Physiology of Ticks* (ed. F. D. Obenchain and R. Galun), pp. 223-244. Elmsford: Pergamon.

Kendall, M. D. (1970). The anatomy of the tarsi of *Schistocerca gregaria* Forskal. *Z. Zellforsch. Mikrosk. Anat.* **109**, 112-137.

Kendall, K. (2001). *Molecular Adhesion and Its Applications - The Sticky Universe*. New York, Boston, Dordrecht, London, Moscow: Kluwer Academic/Plenum Publishers.

Kshirsagar, S. V., Singh, B. and Fulari, S. P. (2009). Comparative study of human and animal hair in relation with diameter and medullary index. *Indian J. Forensic Med. Pathol.* **2**, 105-108.

Labonte, D., Williams, J. A. and Federle, W. (2014). Surface contact and design of fibrillar 'friction pads' in stick insects (*Carausius morosus*): mechanisms for large friction coefficients and negligible adhesion. *J. R. Soc. Interface* **11**, 20140034.

Lees, A. D. (1948). The sensory physiology of the sheep tick. *J. Exp. Biol.* **25**, 145-208.

Lees, A. D. (1969). The behaviour and physiology of ticks. *Acarologia* **11**, 397-410.

Lees, A. M. and Hardie, J. (1988). The organs of adhesion in the aphid *Megoura viciae*. *J. Exp. Biol.* **136**, 209-228.

Leonovich, S. A. (2010). The tarsal gland of ixodid ticks *Ixodes persulcatus* and *Ixodes ricinus* (Mesostigmata, Ixodidae). *Entomol. Rev.* **90**, 1095-1100.

Liebisch, A. and Liebisch, G. (2003). Biologie und Ökologie der Zecken. In *Zeckenborreliose – Lyme-Krankheit bei Mensch und Tier* (ed. H. Horst), pp. 32-48. Balingen: Spitta Verlag GmbH.

MacLeod, J. (1932). The bionomics of *Ixodes ricinus* L., the "sheep tick" of Scotland. *Parasitology* **24**, 382-400.

Michels, J., Appel, E. and Gorb, S. N. (2016). Functional diversity of resilin in Arthropoda. *Beilstein J. Nanotechnol.* **7**, 1241-1259.

Niederegger, S. and Gorb, S. (2003). Tarsal movements in flies during leg attachment and detachment on a smooth substrate. *J. Insect Physiol.* **49**, 611-620.

Nilsson, A. and Lundqvist, L. (1978). Host selection and movements of *Ixodes ricinus* (Acari) larvae on small mammals. *Oikos* **31**, 313-322.

Ohler, A. (1995). Digital pad morphology in torrent-living ranid frogs. *Asiatic Herpetol. Res.* **6**, 85-96.

Oliver, J. H., Jr (1989). Biology and systematics of ticks (Acari: Ixodida). *Annu. Rev. Ecol. Syst.* **20**, 397-430.

Pagenstecher, H. A. (1861). *Beiträge zur Anatomie der Milben. Heft II. Ixodes ricinus*. Leipzig: Verlag von Wilhelm Engelmann.

Peressadko, A. and Gorb, S. N. (2004). Surface profile and friction force generated by insects. In *First International Industrial Conference Bionik, 2004* (ed. I. Boblan and R. Bannasch), pp. 257-261. Düsseldorf: VDI-Verlag.

Perez Goodwyn, P., Peressadko, A., Schwarz, H., Kastner, V. and Gorb, S. (2006). Material structure, stiffness, and adhesion: why attachment pads of the grasshopper (*Tettigonia viridissima*) adhere more strongly than those of the locust (*Locusta migratoria*) (Insecta: Orthoptera). *J. Comp. Physiol. A* **192**, 1233-1243.

Perret, J.-L., Guerin, P. M., Diehl, P. A., Vlimant, M. and Gern, L. (2003). Darkness induces mobility, and saturation deficit limits questing duration, in the tick *Ixodes ricinus*. *J. Exp. Biol.* **206**, 1809-1815.

Rantala, M. J. (1999). Human nakedness: adaptation against ectoparasites? *Int. J. Parasitol.* **29**, 1987-1989.

Rantala, M. J. (2007). Evolution of nakedness in *Homo sapiens*. *J. Zool.* **273**, 1-7.

Reinhardt, K. and Siva-Jothy, M. T. (2007). Biology of the bed bugs (Cimicidae). *Annu. Rev. Entomol.* **52**, 351-374.

Roth, L. M. and Willis, E. R. (1952). Tarsal structure and climbing ability of cockroaches. *J. Exp. Biol.* **119**, 483-517.

Ruser, M. (1933). Beiträge zur Kenntnis des Chitins und der Muskulatur der Zecken (Ixodidae). *Ztschr. Morphol. Ökol. Tiere* **27**, 199-261.

Sauer, J. R., McSwain, J. L., Bowman, A. S. and Essenberg, R. C. (1995). Tick salivary gland physiology. *Annu. Rev. Entomol.* **40**, 245-267.

Scherge, M. and Gorb, S. N. (2001). *Biological Micro- and Nanotribology*. Berlin: Springer.

Schmalfuss, G. (1994). Charakterisierung der physikalischen und chemischen Stimuli für die Wirtserkennung von ixodiden Zecken (*Boophilus microplus* und *Ixodes ricinus*). PhD thesis, Friedrich-Alexander-Universität Erlangen-Nürnberg.

Scholz, I., Baumgartner, W. and Federle, W. (2008). Micromechanics of smooth adhesive organs in stick insects: pads are mechanically anisotropic and softer towards the adhesive surface. *J. Comp. Physiol. A* **194**, 373-384.

Schwartz, G. G. and Rosenblum, L. A. (1981). Allometry of primate hair density and the evolution of human hairlessness. *Am. J. Phys. Anthropol.* **55**, 9-12.

Schwarz, H. and Gorb, S. (2003). Method of platinum-carbon coating of ultrathin sections for transmission and scanning electron microscopy: An application for study of biological composites. *Microsc. Res. Techn.* **62**, 218-224.

Snodgrass, R. E. (1956). *Anatomy of the Honey Bee*. Ithaca, NY: Cornell University Press.

Sonenshine, D. E. and Roe, R. M. (2014a). *Biology of Ticks*, Vol. 1. 2nd edn. Oxford, New York: Oxford University Press.

Sonenshine, D. E. and Roe, R. M. (2014b). *Biology of Ticks*. Vol. 2. 2nd edn. Oxford, New York: Oxford University Press.

Spurr, A. R. (1969). A low-viscosity epoxy resin embedding medium for electron microscopy. *J. Ultrastr. Res.* **26**, 31-43.

Uspensky, I., Ioffe-Uspensky, I., Mumcuoglu, K. Y. and Galun, R. (1999). Body weight characteristics of some ixodid ticks: reflecting adaptations to conditions of their habitats? In *Ecology and Evolution of the Acari* (ed. J. Bruin, L. P. S. van der Geest and M. W. Sabelis), pp. 657-665. Dordrecht: Kluwer Academic Publishers.

Varenberg, M. and Gorb, S. N. (2009). Hexagonal surface micropattern for dry and wet friction. *Adv. Mat.* **21**, 483-486.

Voigt, D. and Gorb, S. (2010). Egg attachment of the asparagus beetle *Crioceris asparagi* to the crystalline waxy surface of *Asparagus officinalis*. *Proc. R. Soc. B* **277**, 895-903.

Voigt, D. and Gorb, S. N. (2012). Attachment ability of sawfly larvae to smooth surfaces. *Arthr. Str. Dev.* **41**, 145-153.

Voigt, D., Gorb, E. and Gorb, S. (2007). Plant surface-bug interactions: *Dicyphus errans* stalking along trichomes. *Arthropod. Plant Interact.* **1**, 221-243.

Voigt, D., Schuppert, J. M., Dattinger, S. and Gorb, S. N. (2008). Sexual dimorphism in the attachment ability of the Colorado potato beetle *Leptinotarsa decemlineata* (Coleoptera: Chrysomelidae) to rough substrates. *J. Insect Physiol.* **54**, 765-776.

Voigt, D., Karguth, A. and Gorb, S. (2012). Shoe soles for the gripping robot: Searching for polymer-based materials maximising friction. *Rob. Auton. Syst.* **60**, 1046-1055.

Voltzit, O. V. (1996). Functional morphology of support-fixation apparatus in the family Ixodidae (Acarina). *Zh. Obshch. Biol.* **57**, 469-489.

Vötsch, W., Nicholson, G., Müller, R., Stierhof, Y.-D., Gorb, S. N. and Schwarz, U. (2002). Chemical composition of the attachment pad secretion of the locust *Locusta migratoria*. *Insect Biochem. Mol. Biol.* **32**, 1605-1613.

Wallade, S. M. and Rice, M. J. (1982). The sensory basis of tick feeding behaviour. In *Physiology of Ticks* (ed. F. D. Obenchain and R. Galun), pp. 71-118. Oxford: Pergamon Press.

Wheeler, P. E. (1985). The loss of functional body hair in man: the influence of thermal environment, body form and bipedality. *J. Hum. Evol.* **14**, 23-28.

Wilhelmsson, P., Lindblom, P., Fryland, L., Nyman, D., Jaenson, T. G. T., Forsberg, P. and Lindgren, P.-E. (2013). *Ixodes ricinus* ticks removed from humans in northern Europe: seasonal pattern of infestation, attachment sites and duration of feeding. *Parasit. Vectors* **6**, 362.

Wohlfart, E., Wolff, J. O., Arzt, E. and Gorb, . S. N. (2014). The whole is more than the sum of all its parts: collective effect of spider attachment organs. *J. Exp. Biol.* **217**, 222-224.

Wolff, J. O. and Gorb, S. N. (2012). Surface roughness effects on attachment ability of the spider *Philodromus dispar* (Araneae, Philodromidae). *J. Exp. Biol.* **215**, 179-184.

Wolff, J. O., Huber, S. J. and Gorb, S. N. (2015a). How to stay on mummy's back: morphological and functional changes of the pretarsus in arachnid postembryonic stages. *Arthr. Str. Dev.* **44**, 301-312.

Wolff, J. O., Seiter, M. and Gorb, S. N. (2015b). Functional anatomy of the pretarsus in whip spiders (Arachnida, Amblypygi). *Arthr. Str. Dev.* **44**, 524-540.

Zurek, D. B., Gorb, S. N. and Voigt, D. (2016). Changes in tarsal morphology and attachment ability to rough surfaces during ontogenesis in the beetle *Gastrophysa viridula* (Coleoptera, Chrysomelidae). *Arthr. Str. Dev.* **46**, 130-137.

Table S1.

Wettability and free surface energy of test substrates**.**

The contact angle measuring device OCAH200 and SCA20 3.7.4 software (Data-Physics Instruments GmbH, Filderstadt, Germany) were used to estimate the wettability of test substrates by contact angle (CA) measurements. The free surface energy (FSE), its polar (p) and disperse (d) portions were calculated. For detailed description of the method see Voigt and Gorb (2010).

Substrate	FSE	Polar component	Disperse component	CA of Aqua millipore water
Substrates used in inversion and traction tests				
Glass	52.4 mN mm^{-1}	36.5 mN mm^{-1}	15.9 mN mm^{-1}	39.3°
Silicone	7.2 mN mm^{-1}	0.5 mN mm^{-1}	6.8 mN mm^{-1}	123°
Spurr resin	27.2 mN mm^{-1}	4.0 mN mm^{-1}	23.2 mN mm^{-1}	91.3°
Native skin*	25-29 mN mm^{-1}	10.8 mN mm^{-1}	16.2 mN mm^{-1}	80-110°
Substrates used in centrifugal force test				
Normal glass	52.0 mN mm^{-1}	34.6 mN mm^{-1}	17.4 mN mm^{-1}	42°
Silanized glass	11.4 mN mm^{-1}	1.8 mN mm^{-1}	9.6 mN mm^{-1}	108°

*according to Ginn et al. (1968); Czech et al. (2011); Persson et al. (2013)

References

Czech, Z., Kowalczyk, A. and Swiderska, J. (2011). Pressure-sensitive adhesives for medical applications. In *Wide Spectra of Quality Control* (ed. I. Akyar), pp. 1-25. Intechopen. doi:10.5772/23827.

Ginn, M. E., Noyes, C. M. and Jungermann, E. (1968). The contact angle of water on viable human skin. *J. Colloid Interface Sci.* **26**, 146-51. doi:10.1016/0021-9797(68)90306-8.

Persson, B. N. J., Kovalev, A. and Gorb, S. N. (2013). Contact mechanics and friction on dry and wet human skin. *Tribol. Let.* **50**, 17-30. doi:10.1007/s11249-012-0053-2.

Voigt, D. and Gorb, S. (2010). Egg attachment of the asparagus beetle *Crioceris asparagi* to the crystalline waxy surface of *Asparagus officinalis*. *Proc. R. Soc. B* **277**: 895-903. doi:10.1098/rspb.2009.1706.

Table S2.

Mean length and width [µm] of leg segments and total legs, *n*=2 per leg number.

Sex	Podomere	L IV Length	L IV Width	L III Length	L III Width	L II Length	L II Width	L I Length	L I Width	Pooled mean Length	Pooled mean Width
F E M A L E	Coxa	333.86	277.84	363.29	245.13	349.54	196.31	350.28	201.26	**349.24**	**230.14**
	Trochanter	347.43	157.44	266.57	169.32	228.82	162.00	209.47	176.78	**263.07**	**166.38**
	Femur	590.99	135.46	418.27	155.08	373.6	145.08	494.45	161.09	**469.33**	**149.18**
	Patella	548.62	156.07	454.52	170.93	381.84	145.48	486.84	162.41	**467.96**	**158.73**
	Tibia	450.39	133.78	370.08	162.41	361.31	143.27	425.99	154.66	**401.94**	**148.53**
	Tarsus	657.74	107.32	561.74	126.70	490.68	127.22	728.01	144.28	**609.54**	**126.38**
	Total leg length	**2929.0**		**2434.5**		**2185.8**		**2695.0**		**2561.1**	
	Mean leg width		161.3		171.6		153.2		166.8		163.2
M A L E	Coxa	138.13	300.78	149.33	252.19	162.08	189.03	215.05	200.67	**166.15**	**235.67**
	Trochanter	140.34	267.09	179.60	162.79	120.14	138.91	178.22	147.38	**154.57**	**179.04**
	Femur	183.33	156.94	313.59	120.25	270.02	120.10	395.83	144.14	**290.69**	**135.36**
	Patella	277.14	136.56	357.21	146.13	272.49	144.35	361.79	158.80	**317.16**	**146.46**
	Tibia	421.21	107.63	256.54	124.14	230.11	133.31	324.61	149.90	**308.12**	**128.75**
	Tarsus	399.07	140.30	442.61	112.02	385.79	129.72	625.90	135.65	**463.34**	**129.42**
	Total leg length	**1559.2**		**1698.9**		**1440.6**		**2101.4**		**1700.0**	
	Mean leg width		184.9		152.9		142.6		156.1		159.1

Table S3.

Area of the pad [μm^2] in contact with a glass slide, while tick is attached to the ceiling. Data on left and right legs are pooled together (mean±standard deviation). Asterisks: statistical differences between unfolded and folded pads for a single leg. Lower case letters: statistical differences between legs I-IV at the same condition (single row). Upper case letters: statistical differences between male and female for a single leg at the same condition.

| Leg no.	I	II	III	IV
Male				
Unfolded	6902.0±1304.28	6581.5±285.59	6348.0±231.61	6837.8±527.09
	A	*, A	*, A	*, A
Expanded	18972.6±294.66	10050.6±186.64	9485.9±1436.81	8885.4±1616.18
	a	b, *	b, *, A	b, *
Female				
Unfolded	10054.4±58.75	9090.9±851.24	7462.8±683.55	9338.5±842.06
	a, B	ab, *, B	b, *, B	a, *, B
Expanded	25237.6±10511.56	13006.1±1234.18	11486.1±178.62	10847.8±514.72
	a	ab, *	b, *, B	b, *

Further results of statistical processing.
Male: expanded pad, differences between legs (one-way ANOVA, $F_{3,9}$=56.2, P<0.001, followed by all pairwise multiple comparison procedure Dunn's test, P<0.05); unfolded vs. unexpanded, leg II (t-test, t=-346, P≤0.001), leg III (t-test, t=-6.2, P≤0.001), leg IV (t-test, t=-2.8, P=0.047).
Female: unfolded pad, differences between legs (one-way ANOVA, $F_{3,21}$=5.6, P=0.006, followed by all pairwise multiple comparison procedure Dunn's test, P<0.05); expanded pad, differences between legs (Kruskal-Wallis one-way ANOVA on ranks, $H_{3,34}$=13.4, P=0.004, followed by all pairwise multiple comparison procedure Dunn's test, P<0.05); unfolded vs. unexpanded condition, leg II (t-test, t=-3.7, P=0.002), leg III (t-test, t=-7.7, P<0.001), leg IV (Mann-Whitney rank sum test, T=58, P=0.022).
Male vs. female: leg I unfolded (Mann-Whitney rank sum test, T=21, P=0.036), leg II unfolded (Mann-Whitney rank sum test, T=34, P=0.035), leg III unfolded (t-test, t=2.6, P=0.021), leg IV unfolded (t-test, t=3.4, P=0.020), leg III expanded (t-test, t=3.0, P=0.020).

Area of the pads in contact, all legs pooled together,

unfolded: 26669 μm^2 in males, 35947 μm^2 in females;

expanded: 47395 μm^2 in males, 60578 μm^2 in females.
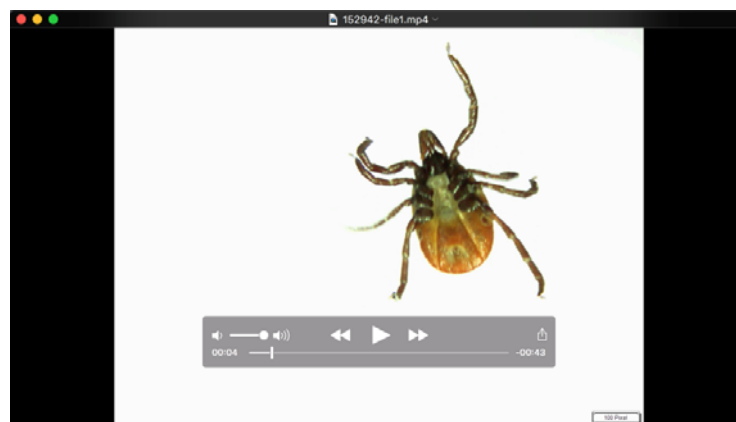
Movie 1.

Females of *Ixodes ricinus* walking on the glass ceiling. Pads while getting in contact and detachment are visible; 3.3 times decelerated.

1st sequence: A female walking on a glass surface at ceiling position.

2nd sequence: Attachment and detachment of translucent adhesive pads during locomotion are visible. The totally expanded adhesive pad of a second leg in contact with a glass surface while tick remained at ceiling position. The process of detachment of the pad is visualized.

3rd sequence: The folded adhesive pad of a foreleg in contact with a glass surface while tick remained at ceiling position. The process of detachment of the pad is visualized. After detachment, a residue of adhesion-mediating fluid is detectable.

4th sequence: The slightly unfolded adhesive pad of a hindleg in contact with a glass surface while tick remained at ceiling position. Tuning of attachment by alteration of the pad area is visible. By pulling the leg, the pad is more folded (claws fold together). By pushing the leg, the pad unfolds while its area increases (claws spread appart).